



ChemComm

**Thermal Management Materials for Energy-Efficient and Sustainable Future Buildings**

Journal:	<i>ChemComm</i>
Manuscript ID	CC-FEA-09-2021-005486
Article Type:	Feature Article

SCHOLARONE™  
Manuscripts

Ref: Invited Paper for the *ChemComm* Emerging Investigators Collection 2021

**Thermal Management Materials for Energy-Efficient and Sustainable Future Buildings**

Zihao Qin, Man Li, Jessica Flohn, Yongjie Hu\*

Department of Mechanical and Aerospace Engineering

University of California, Los Angeles, Los Angeles, CA 90095, USA

\*Corresponding Email: [yhu@seas.ucla.edu](mailto:yhu@seas.ucla.edu)

---

**Abstract:** Thermal management plays a key role in improving the energy efficiency and sustainability of future building envelopes. Here, we focus on the materials perspective and discuss the fundamental needs, current status, and future opportunities for thermal management of buildings. First, we identify the primary considerations and evaluation criteria for high-performance thermal materials. Second, state-of-the-art thermal materials are reviewed, ranging from conventional thermal insulating fiberglass, mineral wool, cellulose, and foams, to aerogels and mesoporous structures, as well as multifunctional thermal management materials. Further, recent progress on passive regulation and thermal energy storage systems are discussed, including sensible heat storage, phase change materials, and radiative cooling. Moreover, we discussed the emerging materials systems with tunable thermal and other physical properties that could potentially enable dynamic and interactive thermal management solutions for future buildings. Finally, we discuss the recent progress in theory and computational design from first-principles atomistic theory, molecular dynamics, to multiscale simulations and machine learning. We expect the rational design that combines data-driven computation and multiscale experiments could bridge the materials properties from microscopic to macroscopic scales and provide new opportunities in improving energy efficiency and enabling adaptive implementation per customized demand for future buildings.

## 1. Introduction

With the increase in global population and living standards, the energy demand in buildings grows continuously<sup>1</sup>. The energy used in buildings accounted for 35% of the world's total energy consumption in 2019, among which residential buildings made up more than 60%,<sup>2</sup> and will further increase by 28% by 2040 according to the U.S. Energy Information Administration<sup>3</sup>. Modern temperature regulation in buildings is mainly achieved through ventilation systems, combined with thermal insulation and storage materials. As illustrated in Figure 1, the energy balance of a building is achieved by thermal contributions from different components and heat transfer routes whose energy efficiency largely depends on the innovative material's design<sup>4,5</sup>. As the total global energy consumption increases dramatically every year<sup>6,7</sup>, it is in critical need to identify fundamental needs and develop advanced thermal management materials to control the heat transfer inside buildings and between the surrounding environments to improve sustainability, energy efficiency, and thermal comfort<sup>8,9</sup>.

Current industrial thermal building materials are mainly focused on thermal insulation<sup>10</sup>, falling under two general categories: (1) inorganic materials (e.g., rocks, ceramics, and glass), and (2) organic materials (e.g., cotton, cellulose, polystyrene, polyurethane, and other polymer foams). Organic materials typically have low thermal conductivities due to weak van der Waals bonding; they usually need to be modified by high mechanically stable fillers to improve the strength<sup>11</sup>. In addition, foams and porous structures have been widely applied to efficiently block heat transfer pathways and further reduce thermal conductivity. In particular, aerogel is a synthetic porous or mesoporous structure derived from a gel by replacing the liquid components with gas while maintaining the gel structure. Various aerogel structures have been investigated from inorganic ( $\text{SiO}_2$ ,  $\text{TiO}_2$ , and  $\text{SiC}$ , etc.) to organic (polyvinyl chloride, polyvinylidene fluoride, polystyrene, cellulose) and carbon aerogels, showing low mass density and thermal conductivity  $\sim 30$  mW/m·K. For practical building applications, multiple properties besides thermal insulation, including lifetime, fire resistance and cost (Figure 2) need to be taken into consideration. For example, manufacturing of ultralight aerogels using facile processing versus high-cost approaches such as super critical drying is important for large scale deployment; other efforts to improve performance of thermal insulation, mechanical strength, reliability, and toxicity are also of importance depending on application targets.

In addition to thermal insulation materials, building thermal management can also be achieved through energy storage technologies<sup>12</sup>. Utilization of available heat sources has been realized by passive thermal energy storage such as using sensible heat of solids or liquids or using latent heat of phase change materials. Despite much progress, challenges exist for the deployment of these storage systems and integration with other thermal management components. For example, passive charge and discharge do not

always coincide with thermal demand periods and ambient temperatures. Developing smart materials that can present not only a simple thermal storage function, but also dynamically control thermal transport for multiple needs could largely improve existing building technologies and enable future thermal management innovations.

This review provides a discussion of identifying the fundamental needs and opportunities in developing advanced thermal management for future buildings from the perspective of material chemistry and physics. We start with identifying the fundamental needs and requirements for sustainable thermal management of buildings, and recent progress in thermal insulation materials. Then we discuss the passive thermal regulation mechanisms and recent progresses, including sensible heat storage materials, phase change materials, and radiative cooling methods highlighted. Further, we highlight the potentials of smart materials with active thermal regulations, including mechanical engineering of building components from static to dynamic thermal system, as well as actively tuning of materials properties. In this end, we discuss recent developments on computational discovery and modeling of materials that can enable effective pathways for discovering new materials. We hope that this review provides readers with a comprehensive perspective on thermal management materials for future buildings and engineering solutions.

## **2. Fundamental needs for sustainable thermal management of buildings**

To meet the growing demand of global energy consumption, the need for improvements in thermal management with a sustainable and high efficiency energy system is becoming more significant. For future engineering design, primary considerations and fundamental needs should be identified. Traditional thermal regulation and energy storage in building elements are usually passive processes and dependent on exterior environments. In this case, thermal properties such as thermal conductivity is the key parameter. However, it poses a challenge for the passive gains and losses of energy to meet the peak demands and thus in the future the energy process could be optimized and made more efficient. For example, smart and active thermal energy storage systems are needed to stock energy when production exceeds demand and to become available when required by users<sup>13</sup>. Other metrics such as efficiency, utilization, lifetime, and capital cost of thermal building materials also need to be evaluated in consideration of the system quality<sup>8</sup>. In Figure 2, we summarize several materials that are currently available and commonly used - including mineral wool<sup>14-18</sup>, expanded polystyrene<sup>14,15,19-21</sup>, extruded polystyrene<sup>15,19,22-24</sup>, polyurethane<sup>15,18,19,25,26</sup>, and aerogel<sup>15,18,19,27,28</sup> - each have limitations in these areas. For example, while aerogel has the most desirable properties in terms of efficiency, vapor resistance, lifetime, fire resistance, and ability to maintain R-value (thermal resistance) with the presence of moisture, the cost is also higher than the other materials.

Polyurethane has the shortest lifetime, highest reduction of R-value with the presence moisture, relatively high degree of fire resistance and thermal resistivity, and lower than average vapor resistance. Optimization over multifunctions could sometimes constitute the major challenge or requirement.

**Efficiency.** To improve thermal management of buildings, a primary area of opportunity for improvement is the efficiency of designs and materials. While a measurement standardization to define the efficiency of thermal management systems has not yet been developed, major topics that contribute to thermal energy conversion or storage efficiency include transport at homogeneous bodies, interfaces, reversibility, and material properties<sup>8</sup>. Today, a primary limitation of thermal insulation is the available materials' thermal conductivity. Ideal insulation materials will have a low thermal conductivity (high thermal resistance). However, the thermal conductivities of materials that are traditionally used in insulation are not low enough that they require large volumes of insulation to meet the energy requirement. This not only occupies building space but also increases cost for materials and installation<sup>8</sup>. To solve the challenge, optimizing energy transport at interfaces is a focus to improve efficiency: As energy is transferred across interfaces between thermal management materials and the heat source or sink, losses occur. The amount of losses that occur depends on thermal resistances. When thermal resistances increase, more energy is required to charge the storage medium. However, there is currently a lack of understanding and predictive models that show the effect of interfaces on transport, partly because resistances are highly geometry dependent. Increasing the understanding of these areas could lead to developments to better control thermal management systems, their efficiency, and performance<sup>8</sup>.

**Utilization.** The utilization of thermal management materials is currently limited by their intrinsic properties. This could be improved through mechanisms to control thermal properties when energy is charged or discharged, or as a function of temperature. Optimal material properties differ greatly according to seasons or other factors, so being able to modify properties to optimize for these conditions would significantly increase utilization<sup>8</sup>. For example, ideal material properties can vary greatly between summer and winter, when rejecting or absorbing more heat from the environment would be advantageous. Material utilization could be improved by developing building blocks with tunable parameters (such as temperature, thermal conductivity, spatial or directional controllability, and thermal storage power density) to adapt the variations in thermal loads or environments. Materials with a dynamically tunable phase transition temperature could benefit certain applications under varied temperatures but currently do not exist. Thermal switches with a tunable thermal conductivity could be used to adjust thermal flow on demand but are currently limited by mechanical design with moving parts; progress has been made in newly approaches using dynamic materials however improvements on the tuning ratio, switching speed, or complexity of external force (field) are needed. In addition to temporal controls, developing thermal elements that enable

directional or anisotropic heat (and mass) transfer<sup>29</sup> would allow the timing of charging and discharging to be determined and greatly increase the utilization. Reliability and lifetime implications of these approaches however need to be investigated.

**Lifetime.** The lifetime of usage is one of the most important aspects of thermal management systems. A longer lifetime allows more useful charge and discharge cycles for the investment of installation. Ideally, the systems should last the lifetime of the building<sup>8</sup>. However, a system's lifetime is often limited by the component barriers that cause the system performance to progressively degrade. For example, many materials currently on the market have thermal conductivities that increase over time under environmental conditions of moisture, humidity, and temperature. Increasing the moisture content of mineral wool from 0 to 10 percent by volume was shown to increase the thermal conductivity from 0.037 to 0.055 W/m·K<sup>30</sup>. Furthermore, materials can be influenced by mass and volume changes, phase decomposition, phase segregation, and corrosion that progressively develop over time, which as a result can reduce energy density, create stresses, and mechanical failure. Using advanced characterization tools to understand and solve issues including slow kinetics, non-equilibrium phases, and poor cyclability could improve the lifetime of thermal management system.

**Capital cost.** Traditional passive thermal regulations - including traditionally thermal mass (e.g., adobe), phase change (e.g., ice storage), and more recently electrochemical (e.g., batteries) - have a high capital cost primarily because of their limited ability to store an impactful amount of energy, necessitating large installations to achieve the required storage<sup>8</sup>. Today, water is the most abundantly used thermal storage material because of its low cost and moderate energy density. However, there is a large room for improvement through the development of new molecules, materials, and chemicals that have high energy and power densities<sup>8</sup>. Nonetheless, for innovations to be practical their production must also be optimized. For example, aerogels offer thermal insulation benefits, but their preparation processing such as supercritical drying can make them more expensive than other commercially available insulation materials. With further refinement, reducing capital cost of these high-performance materials could promote their large-scale deployment.

### 3. Thermal insulation materials

Thermal insulation materials are the most prototype building blocks used in buildings to control heat dissipation rate and temperature. We discuss current industrial thermal insulation materials including mineral wool, fiberglass, foam and other commonly used building blocks. We also review aerogels with

varied compositions and properties promising for extreme thermal insulating applications. Moreover, we discuss recent development of multifunctional thermal insulators that can provide targeted applications such as for transparent windows.

### 3.1 Traditional thermal insulators

Traditional thermal insulation materials include two main categories: (1) inorganic fibrous materials (fiberglass, and mineral wool, etc.), and (2) organic fibrous or foamy materials (cellulose, natural fibers, polystyrene, polyurethane, and phenolic foam, etc.)<sup>10,31</sup>. They account for 60% and 27% of the current market, respectively<sup>32</sup>. We summarized the thermal conductivities of these representative thermal insulation materials in Figure 3: Those extensively used building construction materials including adobe, glass, and concrete, have thermal conductivities typically higher than 0.5 W/m·K; for polyurethane foam<sup>33</sup>, polystyrene foam<sup>34</sup>, mineral wool<sup>35</sup>, cellulose<sup>36</sup> and fiberglass<sup>37</sup>, thermal conductivities are further reduced to be below 0.1 W/m·K but typically above 0.03 W/m·K. While super thermal insulation could benefit certain applications and energy efficiency, under ambient conditions it remains challenging to reduce thermal conductivity to be much lower than 0.03 W/m·K.

**Fiberglass.** Fiberglass, also called glass wool, is the most common and popular insulation material of low cost. It is usually made of a mixture of woven silicon, glass, sand, and other minerals through pultrusion process<sup>38</sup>, which are heated together until melted and then fibers are formed through a spinning machine. In addition to a low thermal conductivity, fiberglass is known to be chemically and thermally stable, and flame retardant. Insulating a house has been deployed with fiberglass board such as in roofs and ceilings<sup>39</sup>. On the other hand, though it is not toxic, safety treatment may be needed for proper usage due to possible tiny shards or powders of glass existing in the product, which can be hazardous to the human lungs, eyes or skin<sup>40</sup>.

**Mineral wool.** Mineral wool is another type of inorganic fibrous thermal insulating material formed by spinning of molten minerals. The manufacturing process of mineral wool is similar to fiberglass, in which the precursors are heated until they are melted and woven together by spinning. Commercially available forms of mineral wool primarily include: (1) rock wool, which is manufactured through natural minerals like basalt or diabase, and (2) slag wool, which comes from blast slag waste<sup>41</sup>. In comparison with fiberglass, mineral wool is advantageous in easy installation and can be cut to a desired shape due to its denser mass. Mineral wool is not combustible and has high melting temperature, therefore is often considered as high

temperature fire-resistant material. For handling, it is usually required to wear safety equipment to avoid skin contact, ingestion or injury.

**Cellulose.** Cellulose is organic fibrous materials and mostly made from recycled paper products such as newsprint, paper, and cardboard followed by a fiberization process. Therefore, cellulose is considered as one of the most environmentally friendly materials. Besides paper fibers, 10-15% of components include inorganic additives for flame retardant purpose such as mineral borate or less expensive boric acid and ammonium sulphate<sup>42</sup>. Cellulose can be densely packed into ceiling and wall cavities in existing homes or loosely filled in unfinished attics. The noticed downsides of cellulose include its tendency to compress over time and absorb water, as well as possible cause of allergies to paper dust.

**Polyurethane foam.** Polyurethane foam is a highly porous organic foamy material fabricated from polyurethane and commonly used to improve insulation for filling areas such as around pipes or small crevices. Polyurethane can be synthesized from various methods and the most common way is copolymerization of di-isocyanate and polyol, such as illustrated in Figure 4A. Polyurethane foam consists of a small portion of polymer to form closed cell structures and a large portion of air within the cells; For some design, replacing air with a lower thermal conductivity gas such as carbon dioxide (CO<sub>2</sub>) and cyclopentane (C<sub>5</sub>H<sub>10</sub>) can further improve insulation performance<sup>43</sup>. To avoid environmental hazard issues to the ozone layer<sup>44</sup>, environmentally friendly non-chlorofluorocarbon foaming agents are used to replace the traditional chlorofluorocarbon or hydrofluorocarbon agents for ceiling and wall insulations. Polyurethane foam has the advantages of being easy applicable into any shapes, e.g., through a spray gun.

**Polystyrene foam.** Polystyrene is a thermoplastic organic foamy material for concrete and structural panel insulations in building envelopes<sup>38,45</sup>. Exemplary polymerization synthesis process of polystyrene from styrene monomers is illustrated in Figure 4B. In the polymerization process, the adjacent C-C  $\pi$  bond in vinyl group is broken to form a new carbon  $\sigma$  bond and attach to a new styrene monomer. Expanded polystyrene and extruded polystyrene are two common polystyrene insulation materials that have been used in building envelopes for decades<sup>46,47</sup>. Expanded polystyrene is produced by expanding polystyrene with gas agents to form small plastic beads, and extruded polystyrene is produced by melting polystyrene and then pressing it through a nozzle to form a porous structure. Similar to PU foam, to achieve flame resistivity, additives are needed. Due to environmental safety issues, traditional additives such as hexabromocyclododecane are replaced by environmentally friendly additives.



### 3.2 Aerogels and mesoporous structures

Aerogels are man-made, highly porous, and low-density solid materials usually formed through drying out the liquid component inside a gel and leaving a porous solid backbone filled up almost entirely by air. Aerogels have many desired properties for building applications including ultralow thermal conductivity, large heat resistance, hardness, chemical stability, thermal stability, and durability, making them promising candidates to improve the sustainability and energy efficiency<sup>48,49</sup>. In addition to aerogels, van der Waals materials<sup>50,51</sup> or mesoporous structures<sup>52</sup> could potentially serve as good thermal insulator. In this part, we review different types of aerogels and mesoporous structures for their thermal properties, structural and mechanical features, etc. which are important parameters in building envelopes.

**Inorganic aerogels.** Inorganic aerogels have been made from oxides, nitrides, metals and carbons, etc., including SiO<sub>2</sub> aerogel<sup>53,54</sup>, BN aerogel<sup>55</sup>, Si<sub>3</sub>N<sub>4</sub> aerogel<sup>56</sup>, and Ag NW aerogel<sup>57</sup>. SiO<sub>2</sub> aerogels and its composites are the earliest and most widely studied (Figure 5A)<sup>53</sup>. The high porous fraction (up to 99%) and low mass density (down to 0.03 g/cm<sup>3</sup>), as well as gas molecular scattering inside small porous structure due to Knudsen effect gives silica aerogels ultralow thermal conductivity ~0.025 W/m·K. However, due to the material's physicochemical properties, silica aerogels constructed by nanoparticle structures are usually fragile and brittle, which limits their current applications<sup>58</sup>. In addition, delicate synthesis process such as supercritical drying, etc. provide manufacturing and cost issues for industrial deployment. Recent developments in additive manufacturing of silica aerogel<sup>59</sup> from aerogel powder in a dilute silica nanoparticle suspension make scalable and low-cost fabrication possible (Figure 5B). To address the low mechanical property issue without affecting thermal insulation properties, efforts have been made in adding additional reinforcement materials including lightweight polymer<sup>60</sup>, fibers<sup>61</sup>, carbon nanotube<sup>62</sup>, and nanowires<sup>63</sup>, etc., in industrial and building insulations. Some elastic and compressible ceramic aerogels have been designed by replacing nanoparticle backbones with flexible nanofiber structures while maintaining low thermal conductivity properties<sup>64</sup>. Inorganic aerogels can also achieve high mechanical strength and modulus as well. For example, a high Young's modulus up to 177.8 MPa has been reported in carbon aerogel using sol-gel polymerization method followed by ambient pressure drying and carbonization<sup>65</sup>. Furthermore, inorganic aerogel has a robust fire resistance and thermal insulation which show high promise for high temperature applications (Figure 5C)<sup>64</sup>. Carbon-based aerogel, as another class of inorganic aerogel, also exhibits flame-retardant properties, which makes them attractive thermal insulation materials as they also exhibit low thermal conductivities<sup>66</sup>.

**Organic aerogels.** Compared to inorganic aerogels, organic aerogels are generally less fragile, more flexible and elastic. Polyvinyl chloride aerogels have been developed through a facile processing under ambient conditions and avoid complication by freeze-drying or supercritical drying. They are preferable for low-cost mass-industrial fabrications<sup>67</sup>. The resulting aerogel exhibited ultralow density, super-flexibility, superhydrophobicity and a low thermal conductivity of 0.028 W/m·K, close to the thermal conductivity of air (Figure 5D). Polyvinylidene fluoride aerogels have been reported using supercritical drying method and showed a comparable performance<sup>68</sup>. Another reported colorless transparent melamine-formaldehyde aerogel<sup>69</sup> showed good thermal insulating performance with improved mechanical properties compared to traditional aerogels with similar density (Figure 5E). On the other hand, organic aerogels have downside in combustion near fire sources. Efforts have been made to improve temperature and flame-retardant performance. For example, Zhao *et al.*<sup>70</sup> reported a renewable polymer-based aerogel to show self-extinguishing performance (Figure 5F).

### 3.3 Multifunctional thermal management materials

Multifunctional materials are desirable for building thermal management, depending on application components. For thermal insulation alone, heat transfer involves different pathways in the forms of conduction, convection and radiations; materials have been desired to suppress these respective heat transfer rates. In addition to thermal insulation, other functionalities such as optical transparency, self-cleaning and noise-isolating could be desired. Developing advanced materials that provide simultaneous control over different physical properties and energy pathways have attracted recent interest and are the key for sustainable buildings in the future.

We use windows technology as an example for discussion in the following. According to U.S. Department of Energy, windows account for a large amount of energy loss in buildings<sup>71</sup>, posing an area of opportunity for thermal management improvement. For better window materials, a combination of high thermal insulation and optical transparency is generally required. In this case, traditional silica aerogel, though an ideal thermal insulation material, is only optically lucid and not of sufficient transparency to be used for windows, not mentioning the unacceptable cost of supercritical drying process. The main reason for the low optical transparency in traditional silica aerogel lies in that the large particle and pore size inside the aerogel backbone leads to strong light scattering and absorption, which reduces the amount of light transmitted through it. A recent study has developed mesoporous silica films with small pore sizes down to ~ 10 nm using polymer template evaporation-induced self-assembly process<sup>72</sup> (Figure 6A). The mesoporous silica films are synthesized to be transparent and uniform. Optical characterization shows highly reduced

light scattering and improved light transmission above 90% with minimized haze<sup>73</sup> while maintains a very low thermal conductivity<sup>74</sup> (Figure 6B). The class of ambient-dried low thermal conductivity mesoporous silica materials enables energy and cost savings through single-pane window design.

Other efforts have been recently made towards the similar goal: Liu *et al.*<sup>75</sup> reported liquid crystalline self-organization cellulose nanofiber aerogel materials<sup>83</sup> to control polymer fibers to cross-link with cellulose fibers into nanostructured lattice-patterned hybrid mesostructures (Figure 6C). Kou *et al.*<sup>76</sup> separated polymer films from each other by air gaps in the framework (Figure 6D). Firth *et al.*<sup>77</sup> deposited thin films composed of silica nanoparticles onto glass through an aerosol-impaction-based process (Figure 6E).

Besides optical transparency, some other multifunctional properties such as superhydrophobic property can also be intriguing for building applications. The reported polyvinyl chloride (PVC) aerogel<sup>67</sup> demonstrated as high as 160° contact angle when contact with water (Figure 5D). Such PVC aerogel processes superhydrophobicity due to its highly porous structure and the weak molecular dipoles of PVC, thus leads to potential for surface engineering and self-cleaning functions. This superhydrophobicity can be very beneficial for building self-cleaning purpose in repelling water, avoiding air moisture absorption and preventing dirty particles adhesion.

#### **4. Passive regulation and thermal energy storage**

Energy can be stored passively in building envelopes for later use to reduce the wasted energy consumption and improve the energy efficiency. Passive regulation has been studied in building engineering for decades and can be incorporated into existing building blocks to reduce the temperature fluctuations and improve the comfort of occupants. Much research has been focused on reducing heat loss or heat gaining via storing thermal energy in sensible heat storage and latent heat storage materials or removing excess energy by radiative cooling techniques. In the following part, we discuss recent progress on these technologies.

##### **4.1 Sensible heat storage**

Thermal energy can be stored in materials as sensible heat without phase change process<sup>78</sup>. As shown in Figure 7A, for sensible heat storage, energy is stored by utilizing the heat capacity of material to absorb heat when temperature increases<sup>79</sup>. The energy storage capacity depends on the specific heat of material, the quantity, density, volume of the materials and the temperature difference. The most

extensively used materials are either in liquid phase, such as water and oils, or in solid phase, such as concrete and ceramics and no phase change is involved in the process<sup>80,81</sup>.

Water and oil are common fluid storage media but are subject to limitations. Water has been one of the most widely used sensible heat storage materials for decades. As shown in Figure 7B, water and aquifer have low density, low cost, high specific heat, and environmentally friendly properties<sup>82</sup>. However, its applications are limited by working temperature between 0 and 100 °C due to intrinsic properties. Oils and molten salts, on the other hand, are appropriate for high temperature applications. Nevertheless, they have lower specific heat and applications are narrowed.

Solid materials, including non-metals and metals, are also commonly used as sensible heat storage materials. Figure 7B shows the typical properties of rock bed, one common solid sensible heat storage material<sup>82</sup>. Compared to liquids, solid materials basically have higher thermal conductivities and a wider operation temperature which can go over 100 °C. They also have better performances in leakage problems. Non-metal solids typically have lower specific heat than liquids. Metals such as copper, aluminum and their alloys have much higher specific heat, and they can store more energy. However, their downside is the high density and high costs in practical applications. Nonmetals such as rocks and concrete have relatively low costs but also low thermal conductivity and specific heat providing less energy storage capacities<sup>83</sup>.

#### 4.2 Phase change materials

Different from sensible heat storage, latent heat storage systems absorb or release thermal energy by means of a material phase change between different states: solid-liquid or liquid-gas (Figure 7A). For practical building thermal applications, only solid-liquid phase transitions are utilized<sup>84</sup>. The capability of absorbing or releasing thermal energy in phase change materials (PCMs) depends on the quantity, latent heat of fusion, and mass of the material. Due to the properties of high energy storage density and the ability to release or absorb heat without temperature changing, PCMs show high promise for efficient thermal storage in practical applications<sup>85,86</sup>. PCMs are typically classified into three categories: inorganic PCMs, organic PCMs, and eutectic PCMs<sup>87</sup>. Figure 7C summarized the properties of some representative PCMs<sup>88</sup>. Phase change materials can be incorporated together with other effective thermal regulation materials into building envelopes for maximizing the thermal energy storage efficiency. As each group has a typical range of melting temperature and melting enthalpy (Figure 7D)<sup>89</sup>, careful evaluations need to be considered for practical performances, including the operation temperature, material heat of fusion and melting point, etc. Drawbacks of phase change material should also be included to evaluate the overall performance.

***Inorganic phase change materials.*** Inorganic PCMs generally have high heat storage capacity, high operation temperatures, and low cost<sup>90</sup>. Hydrated salts and metals<sup>91</sup> are two kinds of compounds that are

typically used in inorganic PCMs. Salt hydrates are generally expressed as  $XY \cdot nH_2O$ , where XY represents the metal salts and n represents the number of water molecules<sup>86</sup>. The solid-liquid phase change is actually achieved by the dehydration and hydration process of the salt. Upon heating, the hydrated salts lose water and dissociate into anhydrous state, while storing energy supplied for dehydration upon heating. Studies have shown the possibility of using salt hydrates for high efficiency thermal energy storage<sup>92</sup>. However, salt hydrates suffer from supercooling issues and corrosive issues, which will lead to a reduction in operation lifetime and storage capacity<sup>93</sup>. Metal PCMs include low melting metals and their eutectic alloys, which perform better in terms of operation lifetime and storage capacity. Besides, they have low toxicity and do not suffer from corrosion, supercooling issues, or large volume changes during phase transition process. Though they are still not ideal for PCMs due to high cost, low heat of fusion and narrowed efficiency<sup>86</sup>, with further developments, they still have potential for thermal storage applications<sup>90,94</sup>.

**Organic phase change materials.** Organic PCMs have many advantages over inorganic PCMs. They are not toxic, not corrosive, chemically stable, and can reversely solidify and melt without phase segregation, which make them promising candidates for thermal energy storage in building elements. The two most studied kinds are paraffin PCMs and non-paraffin PCMs. Paraffin PCMs are composed of straight chain alkane mixture n-alkenes ( $CH_3-CH_2-CH_3$ ). The latent heat of fusion and melting point is dependent on chain length and it will increase with chain length. For example, the melting point of paraffin varies from -12 to 71 °C with different chain lengths and the heat stored can change from 128 to 198 J/g<sup>95</sup>. However, paraffin is not flame-retardant and not compatible with plastics. Furthermore, the low thermal conductivity of paraffin around 0.2 W/m·K narrows possible practical applications<sup>96</sup>. There are numerous types of non-paraffin PCMs that are suitable for building applications, including fatty acids, esters and glycols<sup>97</sup>, which have varying properties due to structure differences. Non-paraffin PCMs can be fabricated from biomaterials, including vegetable oils and animal fats, and are thus considered biodegradable, sustainable, and nontoxic. Non-paraffin PCMs exhibit many advantages such as high latent heat and different melting points. They are appropriate for thermal energy storage in different building conditions<sup>98</sup>.

**Eutectic phase change materials.** Eutectic PCMs are composed of a combination of two or more low melting point PCMs. They can be composed of inorganic PCMs, organic PCMs or a combination of them. When the materials are mixed and frozen, eutectic PCMs are achieved. By altering the ratio of each component in the eutectic PCMs, it is possible to control the intrinsic properties of the system including thermal conductivity, latent heat of fusion, phase change temperature, melting point and density<sup>86,99</sup>. A specially designed PCMs can be promising for efficient thermal energy storage in practical applications.

### 4.3 Radiative cooling

For most buildings, absorption of solar radiation leads to increased requirements of cooling that is currently accomplished through air-conditionings. One developing approach is to modify the radiative surfaces on buildings, such as through radiative cooling, to reflect the solar energy and enhance the radiative energy emission<sup>100</sup>. The idea is to create ideal emissivity for daytime radiative cooling based on solar spectrum and atmospheric transmission spectrum for visible to infrared light (Figure 8A). Normally, buildings under sunshine keep receiving solar radiation energy while emitting infrared light to environments (Figure 8B). Essentially, most radiative cooling design is to minimize the absorptivity of solar spectrum around 500 nm while maximize the emissivity of building thermal radiation around 10  $\mu\text{m}$ . Studies during the past decades have provided different approaches based on metamaterials and photonic structures: For example, Raman and Fan *et al.*<sup>101</sup> reported the planar photonic device with a 5 °C cooling reduction during the daytime under the sun. The device is made of a 1D alternating multilayer of  $\text{HfO}_2$ ,  $\text{SiO}_2$  with different thicknesses on Ag/Si substrate and achieved a 97% of incident solar reflection (Figure 8C). The radiative coolers under sunshine have lower temperature rise than aluminum, black paint or ambient air (Figure 8H). Hossain *et al.*<sup>102</sup> used an array of conical shaped anisotropic metamaterials consisting of multilayers Ge and Al (Figure 8D). Zhai *et al.*<sup>103</sup> reported hybridized nanoparticle embedded polymer film composites (Figure 8E). By taking advantage of the strong phonon-polariton resonance at 9.7  $\mu\text{m}$ , the emissivity around 10  $\mu\text{m}$  of the composite film was close to 1 as shown in Figure 8G. Porous material systems have been applied to maximize solar scattering and improve cooling power<sup>104,105</sup>: Mandal *et al.*<sup>106</sup> designed a hierarchically porous polymer system to maximize the solar light scattering to achieve a cooling power of 96  $\text{W}/\text{m}^2$  as shown in (Figure 8F),

### 5. Dynamic thermal management in buildings

Materials with dynamically tunable thermophysical properties have been proposed to replace or complement static thermal materials due to their adaptivity to the dynamic nature of environment or the varying electrical grid load<sup>8,107</sup>. The U.S. Department of Energy's Building Technologies Office used Energy Management System to evaluate the energy consumption of US residential buildings with thermal energy storage system and dynamical thermal managements of different tunability<sup>107</sup>. The simulations result in Figure 9A showing up to 70% energy consumption in Los Angeles. The potential energy savings from dynamic thermal management of US residential buildings have been comprehensively evaluated by Menyhart *et al.*<sup>108</sup>. In their model, the insulation performance of a wall can be dynamically switched between a conductive state when heat transfer between indoors and outdoors is desired and an insulative

state when heat transfer is not desirable. According to the simulation results as illustrated in Figure 9B, the overall cost savings are highly dependent on the climate of each area, ranging from \$2.84 /m<sup>2</sup> in El Paso, TX up to \$13.62 /m<sup>2</sup> in Fairbanks, AK. These modeling predictions expect a large room using dynamic thermal management for energy savings of buildings and motivated the development of dynamic thermal materials and devices. With the intensive efforts during the last decade, there emerged some options for future dynamical thermal management systems in buildings. But much more research is needed for their practical applications in buildings. For example, the phase change materials with tunable phase transition temperature do not exist yet, however could be one of the most desired building materials<sup>8</sup>.

### **5.1 Electrochromic materials**

The transmittance of solar light is a key factor for the temperature regulation in buildings that can be adjusted through electrochromic properties. Smart windows with adjustable throughput of solar light can reduce energy consumption<sup>109</sup>. Electrochromic materials have been developed and commercially available to dynamically control optical properties under voltage or current since the first demonstration for building windows around forty years ago<sup>110,111</sup>. The transparency contrast of left and right windows in Figure 10A illustrates the optical tunability of electrochromic windows<sup>112</sup>. In a typical electrochromic device as illustrated in Figure 10B, a transparent electrolyte is sandwiched by two oxide films, for example tungsten oxide and nickel oxide<sup>113</sup>. During ion insertion into WO<sub>3</sub>, the electrons change the valence of tungsten atoms and hence become optically absorptive, leading to more than three times optical transmittance of visible light as shown in Figure 10B. During the last decade, nanostructures and nanomaterials have been incorporated into electrochromic devices<sup>114</sup>. For example, low dimensional tungsten oxides were used for improving the optical transmittance tunability and switching speed cost<sup>115-117</sup>. Nanochannels in metal-organic frameworks were used to enhance the ion diffusion and switching speed, stability and enable multicolor switching<sup>118</sup> as shown in Figure 10C. The electrochromic windows can be expected to become more popular in future with further cost reductions.

### **5.2 Mechanical engineering of building components from static to dynamic thermal system**

Heat transfer can also be mechanically modulated by altering the solid contact, fluid density and velocity, and surface geometries. According to the different modulation mechanisms, the mechanical engineering based dynamic thermal system can be categorized as vacuum thermal insulation, mechanical contact thermal switch and heat convection based switchable insulation.

By pressurizing and evacuating gas molecules in an enclosure, the heat transfer rate can be reversibly tuned. Except in the case of radiative thermal transport, heat transfer is always accomplished via

a certain medium. If the medium is removed, such as in vacuum thermal insulation, heat conduction and heat convection cannot occur. As shown in Figure 10D, a typical vacuum thermal insulation system consists of a sealed enclosure and a vacuum pump system<sup>119</sup>. The key to increase the tunability of vacuum thermal insulation systems is to reduce the characteristic size of the enclosure to make the Knudsen effect strong. In other words, only if the characteristic size is comparable with or smaller than mean free path of gas molecules would the thermal conductivity be sensitive to pressure. The main drawback of this technique for buildings is the extra energy consumption of vacuum pumping systems.

Mechanically controlling the contact between two moving objects is another traditional way to manipulate heat transfer as heat conduction over solid or liquid is usually higher than gas and vacuum. A typical mechanical contact thermal switch system requires two polished solid surfaces, an actuator for mechanical movement as illustrated in Figure 10D<sup>119</sup>. For example, the wax actuated thermal switch for NASA aerospace project demonstrated 25 times thermal conductance change using paraffin and metal as two objects and temperature induced thermal expansion as an actuator<sup>120</sup>. By integrating with microelectromechanical systems, the mechanical contact thermal switch can be more accurately controlled with high spatial resolution. Cha *et al.* took advantage of the actuation of liquid droplets in an electro-wetting-on-dielectric configuration (Figure 10E)<sup>121</sup>.

Heat convection happens via a fluid medium, so modifying the fluid characteristics can provide thermal management benefits. By controlling the pressure, flow rate, flow directions, the heat convection can be tuned for buildings. Dabbagh *et al.* developed insulation layers that can synchronously rotate within a wall cavity<sup>122</sup> and modify thermal conductance by gradually rotating the angle. In some cold areas, the buildings are warmed by heat exchanging with hot fluid or gas flow in pipes. Controlling the fluid flow rate in pipes is a popular way to tune heat exchange rates. New methods through altering the turbulence of fluids in pipes were also developed to tune the heat convection. For example, by applying electromagnetic fields across the liquids, the heat transfer rate can be improved by a factor of 20<sup>123</sup>.

There are other types of mechanical engineering based dynamic thermal devices, such as suspended particles<sup>124,125</sup> and phase-change technologies<sup>119,126</sup>. However, the versatility of mechanically engineered dynamic thermal systems needs to consider their design complexity, footprint size, structural shape and working principles.

### 5.3 Dynamic tuning of intrinsic properties of materials

Dynamic tuning of intrinsic material properties has been investigated recently, and we expect that future development in this area may lead to useful materials blocks for building thermal management.



During the last decades, material properties under electric field, temperature, and other stimulation have been studied, though most are fundamental studies in prototyped materials systems.

Ionic motions have been the most prototype approach in modifying microscopic materials structures and modulating physical properties. Ionic interaction has long been investigated for superconductivity<sup>127</sup> and widely used in lithium-ion batteries. Recently, ionic interaction has been applied to layered materials (black phosphorus) and the in situ thermal transport characterization has been performed to determine continuous changes in thermal conductivity by a factor over 6 times (Figure 10F)<sup>128</sup>. The in-situ intercalation process was found to be involved with lattice phase change and ion-phonon interactions that affects thermal transport as a function of ion concentrations. Similar electrochemical modulation of thermal conductance was also observed in other materials<sup>129</sup>. Lu *et al.*<sup>130</sup> took advantage of the tri-phase change of strontium cobalt oxide from perovskite, brownmillerite to hydrogenated phase and measured thermal conductivity change (Figure 10G). The physical implementation of ionic intercalation for building envelopes however needs further development. Current intercalation materials usually need liquid electrolytes while solid states are usually preferred for buildings. The thermal conductivity tuning rate is due to the slow ion diffusion.

The structural change of materials under external stimuli have also been investigated to tune thermal conductivity. Phase change of materials with temperature is well known for altering physical properties. For building envelopes, the temperature triggered thermal switch needs to work near room temperature and maintain their mechanical strength. For example, vanadium dioxide (VO<sub>2</sub>) shows metal–insulator phase transition near room temperature that does not lose much mechanical strength. The changes in both thermal conductivity and emissivity through phase change can be used for thermal management in buildings. The thermal conductivity and emissivity change and transition temperature of VO<sub>2</sub> can be altered with tungsten doping as demonstrated by Lee *et al.*<sup>131</sup> and Tang *et al.*<sup>132</sup>, respectively, which gave a large flexibility of application scenarios. Polymers could also serve as thermal switch materials near room temperature. Shrestha *et al.*<sup>133</sup> demonstrated ten times change of thermal conductivity of crystalline polyethylene nanofibers. The reduction of thermal conductivity was due to the introduction of rotational disorder at high temperature. The structural change of polymer was also observed under light excitation by Shin *et al.*<sup>134</sup>. The azobenzene polymer experienced a reversible conformational transition between trans and cis azobenzene groups (Figure 10H) which leads to a thermal conductivity change from 0.35 to 0.1 W/m·K.

Another aspect in control heat transfer is via radiation. In particular, heat transfer rate was found to depend significantly on the separation distance in near field regime<sup>135,136</sup>. The heat transfer rate can be enhanced up to several orders when the separation distance of two objects is reduced from several  $\mu\text{m}$  to

less than 100 nm<sup>136,137</sup> as shown in Figure 10I. Thus, there exists a large space for thermal regulation using near-field radiation. For example, Thompson *et al.*<sup>138</sup> demonstrated five times change of radiative heat transfer between two coplanar SiN membranes by controlling the distance between them with a third planar object. The response time of their device reached less than 100 s. However, challenge of this approach lies in its manufacturing and the adaption into building structures.

## 6. Computational and data-driven design for materials discovery

With the rapid development of computer hardware and modelling packages from electronic structures to heat transfer at a macroscopic scale, the prediction and fast screening of promising materials and heat transfer performance evaluation in buildings has become possible<sup>139-141</sup>. Moreover, the movement of heat carriers in different nano- or micro-structures can be directly simulated through these advanced modelling techniques, enabling thermal conductivity prediction for composites and porous materials<sup>142-144</sup>. Combined with artificial intelligence algorithms and existing continuum mechanics and finite elements analysis, the multiscale simulation of heat transfer in buildings can be set up. On the other hand, building thermal load prediction can be predicted from machine learning algorithms and used for active optimization of energy consumption<sup>145</sup>. Currently, the automated high-throughput thermal materials screening is mainly focused on homogenous materials. However, it can be expected that more attention would be attracted to automated computational discovery for heterogeneous building materials, motivated by the urgent energy saving demand of buildings. A database of accurately calculated and experimentally measured thermophysical properties for heterogeneous materials should be summarized to assist a machine learning training set. On the other hand, multiscale modelling packages should be developed for easy implementation of accurate thermal conductivity calculation of building insulation materials.

### 6.1 Atomistic modelling of homogeneous thermal materials

During last decades, computational approaches based on atomistic theory from first principles have been developed to reliably determine thermal properties, in addition to continuing models. Atomic force constants can be derived by density functional theory (DFT), density functional perturbation theory and other open-source packages for these calculations<sup>146-150</sup>. For example, by performing DFT calculations of structure patterns with slight displacement of atoms from their equilibrium positions, the second order force constants can be extracted to construct the dynamical matrix and derive the phonon dispersion relationship<sup>139,151,152</sup>. Furthermore, the higher order anharmonicity information can also be extracted from first principles calculation, such as third order, fourth order and even higher order force constants. From

Fermi's golden rule, the multi-phonons scattering rates can be derived from force constants. The power of this modelling technique had been exemplified by the recent discovery and applications of new ultrahigh thermal conductivity materials<sup>153–156</sup>. The agreement with experimental measurements exemplified the power of first principles calculation in new materials discovery. Figure 11A summarized the first principles thermal transport calculation of different materials with six orders of thermal conductivity difference since 2007<sup>141</sup>. However, the large computational resource consumption makes DFT calculations formidable to materials with less periodicity, like alloy and disordered materials. Molecular dynamics (MD) simulation requires much less computational resources by relying on empirical potentials. Thus, the vibrational modes in amorphous materials and total thermal conductivity can be computed from MD simulations. The contribution of propagating, diffusive and localized vibrational modes to thermal transport in amorphous silica can be calculated by Larkin *et al.*<sup>157</sup> and Seyf *et al.*<sup>158</sup> using MD simulations. The physical insight into thermal transport from these techniques and their own predictive capability hold high promise for ultralow thermal conductivity materials screening.

## 6.2 Thermal transport modelling of heterogeneous materials

Most building materials have complicated structures including porosity, nanostructures, interfaces and so on. For example, heat transfer in aerogels includes heat conduction through solid framework, heat convection of gas molecules filled in pores, heat radiation at the surface of solid network, thermal conductance through interfaces<sup>67,159–163</sup>. Transitionally, these different mechanisms can be modelled with classic analytic equations and geometric analysis, though not accurately enough<sup>163,164</sup>. More recently, the MD simulations became available for porous structures. Coquil *et al.*<sup>144</sup> simulated the thermal conductivity of nanoporous silica aerogel using MD simulations to reveal strong size effects, which was later confirmed in their following experimental work<sup>165</sup>. In terms of thermal transport across interfaces, there are several modelling methods, including radiation limit, acoustic mismatch model, diffuse mismatch model, MD simulations, and atomistic Green's function, to name a few<sup>166,167</sup>. By making assumption of the phonon scattering at the interface<sup>161</sup>, the thermal conductance can be calculated from Landauer-Büttiker formulation<sup>168</sup>. In a recent study of heat dissipation in high power transistors, the comparison between experimental measurement of metal-semiconductor interfaces and different modelling techniques showed that MD simulation is more accurate than diffuse mismatch or radiation limit models<sup>156</sup> (Figure 11B). When the targeted modelling system is more than micrometers, Monte Carlo simulation can serve as a powerful tool. Kang *et al.*<sup>142,156</sup> simulated the phonon transport in a microstructure using Monte Carlo simulation and revealed the ballistic transport effects on heat dissipation of a transistor as shown in Figure 11C. Zhao *et al.*<sup>169</sup> adopted Monte Carlo method to study the radiative heat transfer of bulk silica aerogel and proposed

that the extinction coefficient should be modified due to small optical length. When the simulation scale goes up to building size from millimeters to meters, continuum models can be applied, including the finite volume and finite elements methods. For example, Cui *et al.*<sup>155</sup> modelled the thermal performance of a BAs/polymer composites using finite element method (Figure 11D). Bartak *et al.*<sup>170</sup> assessed the thermal comfort and air quality by simulating the thermal and fluid fields in buildings with computational fluid dynamics as shown in Figure 11E.

### 6.3 Machine learning assisted high throughput thermal materials discovery

The discovery of high throughput materials via machine learning is evolving into an important strategy for accelerating materials design, synthesis, characterization, and application in the future<sup>171,172</sup>, including for thermal materials<sup>173–175</sup>. In a machine learning screening, the materials with desired properties are assessed from the correlation between materials descriptors and targeted material properties<sup>176</sup>. The database of first principles or molecular dynamics calculated or experimentally measured thermal conductivity and other easy-to-evaluate materials descriptors should be established, such as bulk modulus, Debye frequencies. Good material descriptors should be developed to correlate them with thermal conductivity via machine learning regression algorithms. Thus, the hard-to-evaluate thermal conductivity can be quickly screened via the easy-to-evaluate material descriptors. Carrete *et al.*<sup>177</sup> found unprecedentedly low thermal conductivity half-Heusler Semiconductors via machine learning algorithms. They evaluated approximately 79,000 half-Heusler materials using AFLOWLIB platform and narrowed down to 995 configurations with minimum enthalpy and further down to 450 mechanically stable structures, and to a final list with 75 entries as shown in Figure 11F. Three low thermal conductivity materials were found according to descriptors-thermal conductivity correlations. Juneja *et al.*<sup>178</sup> discovered 15 ultrahigh and ultralow thermal conductivity materials from 195 compounds using Gaussian process regression-based machine learning and simple descriptors, namely, maximum phonon frequency, integrated Grüneisen parameter, average atomic mass, and volume of the unit cell. Chowdhury *et al.*<sup>179</sup> predicted aperiodic superlattice structures with the lowest thermal conductivity by maximizing Anderson localization of phonons using a genetic algorithm-based approach as illustrated in Figure 11G. The interfacial thermal resistance can also be predicted from machine learning method by selecting appropriate descriptors<sup>180</sup>.

## 7. Future perspectives

In the present review, we focused on the materials perspective and comprehensively discussed recent progress on thermal materials for building engineering. We reviewed the fundamental needs, the

state-of-the-art materials, and future possibilities to improve building's energy efficiency and sustainability, from thermal insulation, thermal energy storage, to multifunctional and dynamic tunable thermal management materials. While passive thermal insulation is the current mainstream, we expect several other forms including dynamic and interactive thermal regulations could play a more important role in future smart and sustainable buildings. To achieve this goal, further development that stems from fundamental research to engineering innovations are needed. The practical deployment for building infrastructures not only requires materials with desired thermal and other physical properties, but also requires the careful consideration in building and structural implementations, such as liquid-free, compact and adaptive structures, cost effective, and large-scale manufacturing, etc. In addition, we expect computer-assisted materials search using hierarchical toolsets from atomistic, to mesoscopic, microscopic and macroscopic scales, together with multiscale experimental characterizations, will play an important role in identifying high-performance materials, or even customizing design to meet specific building requirements. We hope this review would provide helpful insights on thermal management materials for future buildings.

## Figure captions

**Figure 1. Illustration of energy balance in a representative building envelope.** (A). Schematic illustration showing the total thermal contributions in a building. (B). Heat dissipation routes and their contribution percentages in a building envelope<sup>4,5</sup>. (C). Global energy consumption from 1920 to 2019, with a forecast to 2040<sup>6,7</sup>.

**Figure 2. Performance comparison of building thermal insulation materials. Prototyped** thermal insulation materials are evaluated using key performance metrics. The analysis results are made using data from literature reports<sup>14-28</sup>.

**Figure 3. Thermal conductivity comparison of traditional building construction materials and representative commercially available thermal insulation materials.** The scanning electron microscopy (SEM) images for commercially available thermal insulation materials are from reference: Polyurethane (PU) foam<sup>33</sup>, Polystyrene (PS) foam<sup>34</sup>, Mineral wool<sup>35</sup>, Cellulose<sup>36</sup>, and Fiberglass<sup>37</sup>.

**Figure 4. Common polymerization synthesis route.** (A) Polyurethane and (B) Polystyrene.

**Figure 5. A summary of aerogels with different properties.** (A). An optical image of Silica-based aerogels and their composites with different properties<sup>53</sup>. (B). Low-cost additive manufacturing of silica aerogels<sup>59</sup>. (C). Ceramic aerogel under high temperature performances<sup>64</sup>. (D). Polyvinyl chloride aerogel showing ultralight, ultra-flexible and superhydrophobic properties<sup>67</sup>. (E). Transparent melamine-formaldehyde aerogel with high mechanical properties<sup>69</sup>. (F). Fiber-reinforced polymer aerogel composites with flame retardant property<sup>70</sup>.

**Figure 6. Representative design strategies for multifunctional thermal management materials.** (A). Synthesis process of small nanoparticle size, transmission electron microscope (TEM) image and<sup>72</sup> a representative optical photograph of the mesoporous silica film<sup>73</sup>. (B). Solid volume fraction-dependent thermal conductivity of the mesoporous silica film<sup>74</sup>. (C). Schematic illustration and an optical image of the liquid crystalline self-organization cellulose nanofiber aerogel<sup>75</sup>. (D). Schematic illustration of the thermal insulating polymer-air multilayer system<sup>76</sup>. (E). Scheme of fabrication process for the nanoparticle-based thin films and a representative SEM image<sup>77</sup>.

**Figure 7. Comparison of sensible heat storage and latent heat storage technologies for passive thermal regulation.** (A). Thermal profile of sensible heat storage and latent heat storage techniques<sup>79</sup>. (B). Comparison of properties of two common types of sensible heat storage materials<sup>82</sup>. (C). Comparison of properties of different types of phase change materials<sup>88</sup>. (D). The melting enthalpy and melting temperature for the different groups of phase change materials<sup>89</sup>.

**Figure 8. Daytime radiative cooling technologies for energy building savings.** (A). An ideal emissivity plot for daytime radiative cooling based on solar spectrum and atmospheric transmission spectrum for visible to infrared light; (B). Radiative heat transfer schematic at the surface of radiative cooling material; (C-H). Representative design strategies and performances for daytime radiative cooling. (C) and (H). Layered material radiative cooler and the comparison of temperature rise to other materials during daytime<sup>101</sup>. (D). Metamaterial radiative cooler<sup>102</sup>. (E) and (G). Composites with nanoparticles radiative cooler and its experimentally measured emissivity property for daytime radiative cooling<sup>103</sup>. (F). Porous materials radiative cooler<sup>106</sup>.

**Figure 9. Evaluation of energy saving and cost reduction of buildings with dynamic thermal management systems in US.** (A). Energy cost savings contour map estimated for US residential buildings with dynamical thermal management<sup>107</sup>. (B). Annual energy consumption of heating, ventilation, and cooling systems with dynamical thermal managements of different tunability<sup>108</sup>.

**Figure 10. Dynamic thermal management systems.** (A). A visual illustration of an office equipped with electrochromic windows, the left and right side of which are in transparent and dark state respectively<sup>112</sup>. (B). An exemplary optical transmission spectrum modulated by charging and discharging of electrochromic device, made of transparent electrolyte, tungsten oxide and nickel oxide<sup>113</sup>. (C). The multicolor performance of metal organic framework based electrochromic device with different voltage<sup>118</sup>. (D). Schematic diagram of vacuum gas gap and mechanical contact based thermal switches<sup>119</sup>. (E). Schematic of a mechanical contact thermal switch based on electro-wetting-on-dielectric technique<sup>121</sup>. (F). Ionic intercalation in black phosphorus for active control of anisotropic thermal conductivity<sup>128</sup>. (G). Thermal conductivity turning of strontium cobalt oxide by controlling oxygen and proton concentration<sup>130</sup>. (H). Light triggered thermal conductivity switching of azopolymer<sup>134</sup>. (I). Tunable thermal energy transport enabled by the distance dependent near-field radiative heat transfer<sup>137</sup>.

**Figure 11. High throughput computational thermal materials discovery and analysis from atomic scale by first principles to macroscale aided by machine learning.** (A). A summary of first principles thermal conductivity calculation of different materials since 2007<sup>121</sup>. (B). Interface phonon transport across metal and semiconductors interface from experiments, and different modelling methods<sup>156</sup>. (C). Hot spot temperature in transistor calculated from Monte Carlo simulations<sup>156</sup>. (D). Thermal transport modelling of a BAs/polymer composites using finite element method<sup>155</sup>. (E). Thermal comfort and air quality evaluation by simulating the thermal and fluid fields in buildings with computational fluid dynamics<sup>170</sup>. (F). Unprecedentedly low thermal conductivity half-Heusler semiconductors screening via machine learning algorithms<sup>177</sup>. (G). Optimization of aperiodic superlattice structures for lowest thermal conductivity using a genetic algorithm<sup>179</sup>.

## References

- 1 U.S. Department of Energy, Heating and Cooling, <https://www.energy.gov/energysaver/heating-and-cooling>.
- 2 IEA and UNEP, 2020 Global Status Report for Buildings and Construction, <https://globalabc.org/resources/publications/2020-global-status-report-buildings-and-construction>.
- 3 U.S. Energy Information Administration, Today in Energy, <https://www.eia.gov/todayinenergy/>.
- 4 E. Anderson, M. Antkowiak, R. Butt, J. Davis, J. Dean and M. Hillesheim, *A Broad Overview of Energy Efficiency and Renewable Energy Opportunities for Department of Defense Installations A Broad Overview of Energy Efficiency and Renewable Energy Opportunities for Department of Defense Installations*, Colorado, 2011.
- 5 Shrink that footprint, Typical Home Heat Gains and Losses, <http://shrinkthatfootprint.com/home-heat-loss>.
- 6 Our World in Data, Global direct primary energy consumption, [https://ourworldindata.org/grapher/global-primary-energy?country=~OWID\\_WRL](https://ourworldindata.org/grapher/global-primary-energy?country=~OWID_WRL).
- 7 Statista, Energy consumption worldwide from 2000 to 2018, with a forecast until 2050\*, <https://www.statista.com/statistics/222066/projected-global-energy-consumption-by-source/>.
- 8 M. Bianchi, S. Kaur and N. James, *2019 Workshop on Fundamental Needs for Dynamic and Interactive Thermal Storage Solutions for Buildings*, United States, 2020.
- 9 O. S. Board and E. National Academies of Sciences and Medicine, *Environmental engineering for the 21st century: Addressing grand challenges*, National Academies Press, 2019.
- 10 U.S. Department of Energy, Insulation Materials, <https://www.energy.gov/energysaver/insulation-materials>.
- 11 A. K. Mohanty, S. Vivekanandhan, J. M. Pin and M. Misra, *Science*, 2018, **362**, 536–542.
- 12 U.S. Department of Energy, Energy Storage Market Report 2020, <https://www.energy.gov/energy-storage-grand-challenge/downloads/energy-storage-market-report-2020>.
- 13 I. Sarbu and C. Sebarchievici, *Solar heating and cooling systems: Fundamentals, experiments and applications*, Academic Press, 2016.
- 14 M. M. Koebel, L. Huber, S. Zhao and W. J. Malfait, *J. Sol-Gel Sci. Technol.*, 2016, **79**, 308–318.



- 15 E. Cohen, *Dr. Diss. Massachusetts Inst. Technol.*, 2011.
- 16 F. Tittarelli, F. Stazi, G. Politi, C. di Perna and P. Munafò, *Int. J. Chem. Environ. Biol. Sci.*, 2014, **1**, 779–783.
- 17 G. Deshmukh, P. Birwal, R. Datir and S. Patel, *J. Food Process. Technol.*, 2017, **8**, 1–5.
- 18 PIMA performance Bulletin, Foil-faced polyiso and unfaced mineral wool board in commercial wall applications,  
[https://cdn.ymaws.com/www.polyiso.org/resource/resmgr/performance\\_bulletins/Mineral\\_Wool\\_PerformBulletin.pdf](https://cdn.ymaws.com/www.polyiso.org/resource/resmgr/performance_bulletins/Mineral_Wool_PerformBulletin.pdf).
- 19 M. Giarrusso, High Performance Thermal Insulation : Silica Aerogels in Construction Technology,  
<https://digitalworks.union.edu/cgi/viewcontent.cgi?article=2157&context=theses>.
- 20 Buildblock, What is the expected lifetime of the expanded polystyrene (EPS) foam?,  
<https://buildblock.com/asked-answered-what-is-the-expected-lifetime-of-the-expanded-polystyrene-eps-foam/>.
- 21 Construction specifier, Comparing Polystyrenes: Looking at the differences between EPS and XPS, <https://www.constructionspecifier.com/comparing-polystyrenes-looking-at-the-differences-between-eps-and-xps/2/>.
- 22 Polystyrene Insulation, High Performance Foam Plastic Rigid Insulation,  
<http://commercial.owenscorning.com/assets/0/144/172/174/e45fe07d-5cc9-4e4b-866a-5e35d75090ec.pdf>.
- 23 M. Davraz and H. C. Bayrakçı, 2 nd International Balkans Conference on Challenges of Civil Engineering, BCCCE, 23-25 May 2013, Epoka University, Tirana, Albania., 2013.
- 24 Airfoam, EPS and XPS Insulation Comparison, <https://www.airfoam.com/EPS-vs-XPS-Foam-Insulation.php>.
- 25 U.S. Cooler, A Matter of Insulation: Acquisition vs. Lifetime Savings,  
<https://www.uscooler.com/blog/insulation-acquisition-lifetime-savings/>.
- 26 Spray Polyurethane Foam Alliance, *Moisture vapor transmission*, 1994.
- 27 Á. Lakatos, *Energy Build.*, 2017, **139**, 506–516.
- 28 R. Nosrati and U. Berardi, *Energy Procedia*, 2017, **132**, 303–308.

- 29 M. Li, J. S. Kang and Y. Hu, *Rev. Sci. Instrum.*, 2018, **89**, 84901.
- 30 B. P. Jelle, *Energy Build.*, 2011, **43**, 2549–2563.
- 31 A. M. Papadopoulos, *Energy Build.*, 2005, **37**, 77–86.
- 32 A. M. Papadopoulos, *Proj. Interim Report, Thessaloniki*.
- 33 H. Shi, D. Shi, L. Yin, Z. Yang, S. Luan, J. Gao, J. Zha, J. Yin and R. K. Y. Li, *Nanoscale*, 2014, **6**, 13748–13753.
- 34 F. Schüler, D. Schamel, A. Salonen, W. Drenckhan, M. D. Gilchrist and C. Stubenrauch, *Angew. Chemie Int. Ed.*, 2012, **51**, 2213–2217.
- 35 C. Siligardi, P. Miselli, E. Francia and M. Lassinantti Gualtieri, *Energy Build.*, 2017, **138**, 80–87.
- 36 T. Li, J. Song, X. Zhao, Z. Yang, G. Pastel, S. Xu, C. Jia, J. Dai, C. Chen, A. Gong, F. Jiang, Y. Yao, T. Fan, B. Yang, L. Wågberg, R. Yang and L. Hu, *Sci. Adv.*, 2021, **4**, eaar3724.
- 37 X. Liu, Y. Wang, Z. Chen, K. Ben and Z. Guan, *Appl. Surf. Sci.*, 2016, **360**, 789–797.
- 38 M. S. Al-Homoud, *Build. Environ.*, 2005, **40**, 353–366.
- 39 K. A. Al-Sallal, *Renew. energy*, 2003, **28**, 603–611.
- 40 T. W. Hesterberg, R. Anderson, D. M. Bernstein, W. B. Bunn, G. A. Chase, A. L. Jankousky, G. M. Marsh and R. O. McClellan, *Regul. Toxicol. Pharmacol.*, 2012, **62**, 257–277.
- 41 B. Blagojevič, B. Širok and M. Hočevar, *Ceramics–Silikáty*, 2009, **53**, 25–30.
- 42 P. L. Hurtado, A. Rouilly, V. Vandenbossche and C. Raynaud, *Build. Environ.*, 2016, **96**, 170–177.
- 43 N. V Gama, A. Ferreira and A. Barros-Timmons, *Materials*, 2018, **11**, 1841.
- 44 K. Stemmler, D. Folini, S. Ubl, M. K. Vollmer, S. Reimann, S. O’Doherty, B. R. Grealley, P. G. Simmonds and A. J. Manning, *Environ. Sci. Technol.*, 2007, **41**, 1145–1151.
- 45 U.S. Department of Energy, Types of insulation, <https://www.energy.gov/energysaver/types-insulation>.
- 46 L. Jiao and J. Sun, *Procedia Eng.*, 2014, **71**, 622–628.
- 47 S. Doroudiani and H. Omidian, *Build. Environ.*, 2010, **45**, 647–654.

- 48 J. Mao, J. Iocozzia, J. Huang, K. Meng, Y. Lai and Z. Lin, *Energy Environ. Sci.*, 2018, **11**, 772–799.
- 49 Q. Zeng, T. Mao, H. Li and Y. Peng, *Energy Build.*, 2018, **174**, 97–110.
- 50 J. S. Kang, H. Wu, M. Li and Y. Hu, *Nano Lett.*, 2019, **19**, 4941–4948.
- 51 H. D. Nguyen, J. S. Kang, M. Li and Y. Hu, *Nanoscale*, 2019, **11**, 3129–3137.
- 52 N. A. Rongione, M. Li, H. Wu, H. D. Nguyen, J. S. Kang, B. Ouyang, H. Xia and Y. Hu, *Adv. Electron. Mater.*, 2019, **5**, 1800774.
- 53 C. A. Morris, M. L. Anderson, R. M. Stroud, C. I. Merzbacher and D. R. Rolison, *Science*, 1999, **284**, 622–624.
- 54 S. S. Prakash, C. J. Brinker, A. J. Hurd and S. M. Rao, *Nature*, 1995, **374**, 439–443.
- 55 X. Xu, Q. Zhang, M. Hao, Y. Hu, Z. Lin, L. Peng, T. Wang, X. Ren, C. Wang and Z. Zhao, *Science*, 2019, **363**, 723–727.
- 56 L. Su, M. Li, H. Wang, M. Niu, D. Lu and Z. Cai, *ACS Appl. Mater. Interfaces*, 2019, **11**, 15795–15803.
- 57 F. Qian, P. C. Lan, M. C. Freyman, W. Chen, T. Kou, T. Y. Olson, C. Zhu, M. A. Worsley, E. B. Duoss and C. M. Spadaccini, *Nano Lett.*, 2017, **17**, 7171–7176.
- 58 K. E. Parmenter and F. Milstein, *J. Non. Cryst. Solids*, 1998, **223**, 179–189.
- 59 S. Zhao, G. Siqueira, S. Drdova, D. Norris, C. Ubert, A. Bonnin, S. Galmarini, M. Ganobjak, Z. Pan and S. Brunner, *Nature*, 2020, **584**, 387–392.
- 60 H. Maleki, L. Durães and A. Portugal, *Microporous mesoporous Mater.*, 2014, **197**, 116–129.
- 61 X. Yang, Y. Sun, D. Shi and J. Liu, *Mater. Sci. Eng. A*, 2011, **528**, 4830–4836.
- 62 M. Piñero, M. del Mar Mesa-Díaz, D. de los Santos, M. V Reyes-Peces, J. A. Díaz-Fraile, N. de la Rosa-Fox, L. Esquivias and V. Morales-Florez, *J. Sol-Gel Sci. Technol.*, 2018, **86**, 391–399.
- 63 L. Su, H. Wang, M. Niu, S. Dai, Z. Cai, B. Yang, H. Huyan and X. Pan, *Sci. Adv.*, 2020, **6**, eaay6689.
- 64 Y. Si, X. Wang, L. Dou, J. Yu and B. Ding, *Sci. Adv.*, 2018, **4**, eaas8925.
- 65 X. Jia, B. Dai, Z. Zhu, J. Wang, W. Qiao, D. Long and L. Ling, *Carbon*, 2016, **108**, 551–560.

- 66 Y. Hanzawa, H. Hatori, N. Yoshizawa and Y. Yamada, *Carbon*, 2002, **40**, 575–581.
- 67 M. Li, Z. Qin, Y. Cui, C. Yang, C. Deng, Y. Wang, J. S. Kang, H. Xia and Y. Hu, *Adv. Mater. Interfaces*, 2019, **6**, 1900314.
- 68 J. Zhang, Y. Kong and X. Shen, *Mater. Lett.*, 2020, **259**, 126890.
- 69 Y. Nakanishi, Y. Hara, W. Sakuma, T. Saito, K. Nakanishi and K. Kanamori, *ACS Appl. Nano Mater.*, 2020, **3**, 49–54.
- 70 H.-B. Zhao, M. Chen and H.-B. Chen, *ACS Sustain. Chem. Eng.*, 2017, **5**, 7012–7019.
- 71 U.S. Department of Energy, Update or Replace Windows,  
<https://www.energy.gov/energysaver/update-or-replace-windows>.
- 72 Y. Yan, S. C. King, M. Li, T. Galy, M. Marszewski, J. S. Kang, L. Pilon, Y. Hu and S. H. Tolbert, *J. Phys. Chem. C*, 2019, **123**, 21721–21730.
- 73 M. Marszewski, S. C. King, Y. Yan, T. Galy, M. Li, A. Dashti, D. M. Butts, J. S. Kang, P. E. McNeil and E. Lan, *ACS Appl. Nano Mater.*, 2019, **2**, 4547–4555.
- 74 D. M. Butts, P. E. McNeil, M. Marszewski, E. Lan, T. Galy, M. Li, J. S. Kang, D. Ashby, S. King and S. H. Tolbert, *MRS Energy Sustain.*
- 75 Q. Liu, A. W. Frazier, X. Zhao, A. Joshua, A. J. Hess, R. Yang and I. I. Smalyukh, *Nano Energy*, 2018, **48**, 266–274.
- 76 R. Kou, Y. Zhong, Q. Wang, J. Kim, R. Chen and Y. Qiao, *Appl. Therm. Eng.*, 2021, **191**, 116890.
- 77 P. Firth and Z. C. Holman, *ACS Appl. Nano Mater.*, 2018, **1**, 4351–4357.
- 78 B. Koçak, A. I. Fernandez and H. Paksoy, *Sol. Energy*, 2020, **209**, 135–169.
- 79 H. Mehling and L. F. Cabeza, *Heat and cold storage with PCM*, Springer, 2008, vol. 308.
- 80 S. Kuravi, J. Trahan, D. Y. Goswami, M. M. Rahman and E. K. Stefanakos, *Prog. Energy Combust. Sci.*, 2013, **39**, 285–319.
- 81 A. Gil, M. Medrano, I. Martorell, A. Lázaro, P. Dolado, B. Zalba and L. F. Cabeza, *Renew. Sustain. energy Rev.*, 2010, **14**, 31–55.
- 82 G. Li, *Renew. Sustain. Energy Rev.*, 2016, **53**, 897–923.
- 83 Y. Tian and C.-Y. Zhao, *Appl. Energy*, 2013, **104**, 538–553.

- 84 X. Sun, Q. Zhang, M. A. Medina and K. O. Lee, *Appl. Energy*, 2016, **162**, 1453–1461.
- 85 H. Nazir, M. Batool, F. J. B. Osorio, M. Isaza-Ruiz, X. Xu, K. Vignarooban, P. Phelan and A. M. Kannan, *Int. J. Heat Mass Transf.*, 2019, **129**, 491–523.
- 86 A. Sharma, V. V. Tyagi, C. R. Chen and D. Buddhi, *Renew. Sustain. energy Rev.*, 2009, **13**, 318–345.
- 87 M. R. Anisur, M. H. Mahfuz, M. A. Kibria, R. Saidur, I. Metselaar and T. M. I. Mahlia, *Renew. Sustain. Energy Rev.*, 2013, **18**, 23–30.
- 88 G. Li, Y. Hwang and R. Radermacher, *Int. J. Refrig.*, 2012, **35**, 2053–2077.
- 89 D. Zhou, C.-Y. Zhao and Y. Tian, *Appl. Energy*, 2012, **92**, 593–605.
- 90 M. Liu, W. Saman and F. Bruno, *Renew. Sustain. Energy Rev.*, 2012, **16**, 2118–2132.
- 91 G. Ferrer, A. Solé, C. Barreneche, I. Martorell and L. F. Cabeza, *Renew. Sustain. Energy Rev.*, 2015, **50**, 665–685.
- 92 O. Al-Abbasi, A. Abdelkefi and M. Ghommem, *Int. J. Energy Res.*, 2017, **41**, 2149–2161.
- 93 H. Liu and H. B. Awbi, *Build. Environ.*, 2009, **44**, 1788–1793.
- 94 W. Su, J. Darkwa and G. Kokogiannakis, *Renew. Sustain. Energy Rev.*, 2015, **48**, 373–391.
- 95 S. Peng, A. Fuchs and R. A. Wirtz, *J. Appl. Polym. Sci.*, 2004, **93**, 1240–1251.
- 96 S. Kamali, *Energy Build.*, 2014, **80**, 131–136.
- 97 M. M. Kenisarin, *Sol. Energy*, 2014, **107**, 553–575.
- 98 A. Sari, *Energy Convers. Manag.*, 2004, **45**, 2033–2042.
- 99 V. V. Tyagi and D. Buddhi, *Renew. Sustain. energy Rev.*, 2007, **11**, 1146–1166.
- 100 X. Lu, P. Xu, H. Wang, T. Yang and J. Hou, *Renew. Sustain. Energy Rev.*, 2016, **65**, 1079–1097.
- 101 A. P. Raman, M. Abou Anoma, L. Zhu, E. Rephaeli and S. Fan, *Nature*, 2014, **515**, 540–544.
- 102 M. M. Hossain, B. Jia and M. Gu, *Adv. Opt. Mater.*, 2015, **3**, 1047–1051.
- 103 Y. Zhai, Y. Ma, S. N. David, D. Zhao, R. Lou, G. Tan, R. Yang and X. Yin, *Science*, 2017, **355**, 1062–1066.
- 104 L. Tian, Z. Yao, H. Shuaiming, G. Wentao, W. Zhiyuan, H. Mohammad, D. Daniel, M. Ruiyu, Z.

- Xinpeng, S. Jianwei, D. Jiaqi, C. Chaoji, A. Ablimit, V. Azhar, M. Ashlie, Y. Ronggui, S. Jelena, Y. Xiaobo and H. Liangbing, *Science*, 2019, **364**, 760–763.
- 105 Z. Shaoning, P. Sijie, S. Minyu, W. Zhuning, W. Maoqi, L. Xinhang, C. Mingyue, X. Yuanzhuo, W. Jiawei, Z. Manni, C. Qingqing, T. Yuwei, Z. Xianheng, H. Zhiheng, W. Rui, T. Alitenai, S. Xiyu, X. Zhigang, T. Mingwei, C. Min, M. Xiao, Y. Lv Yun, Z. Jun, Z. Huamin, Y. Qing, L. Xin, M. Yaoguang and T. Guangming, *Science*, 2021, **373**, 692–696.
- 106 J. Mandal, Y. Fu, A. C. Overvig, M. Jia, K. Sun, N. N. Shi, H. Zhou, X. Xiao, N. Yu and Y. Yang, *Science*, 2018, **362**, 315–319.
- 107 S. Mumme, N. James, M. Salonvaara, S. Shrestha and D. E. Hun, *Smart and Efficient Building Envelopes: Thermal Switches and Thermal Storage for Energy Savings and Load Flexibility*, Oak Ridge National Lab.(ORNL), Oak Ridge, TN (United States), 2020.
- 108 K. Menyhart and M. Krarti, *Build. Environ.*, 2017, **114**, 203–218.
- 109 E. Lee, M. Yazdanian and S. Selkowitz, *The energy-savings potential of electrochromic windows in the US commercial buildings sector*, Ernest Orlando Lawrence Berkeley National Laboratory, Berkeley, CA (US), 2004.
- 110 J. Svensson and C. G. Granqvist, *Sol. energy Mater.*, 1984, **11**, 29–34.
- 111 C. M. Lampert, *Sol. Energy Mater.*, 1984, **11**, 1–27.
- 112 C. G. Granqvist, *Thin Solid Films*, 2016, **614**, 90–96.
- 113 I. B. Pehlivan, R. Marsal, E. Pehlivan, E. L. Runnerstrom, D. J. Milliron, C. G. Granqvist and G. A. Niklasson, *Sol. energy Mater. Sol. cells*, 2014, **126**, 241–247.
- 114 G. Yang, Y.-M. Zhang, Y. Cai, B. Yang, C. Gu and S. X.-A. Zhang, *Chem. Soc. Rev.*, 2020, **49**, 8687–8720.
- 115 Y. Li, W. A. McMaster, H. Wei, D. Chen and R. A. Caruso, *ACS Appl. Nano Mater.*, 2018, **1**, 2552–2558.
- 116 S. Lee, R. Deshpande, P. A. Parilla, K. M. Jones, B. To, A. H. Mahan and A. C. Dillon, *Adv. Mater.*, 2006, **18**, 763–766.
- 117 A. Azam, J. Kim, J. Park, T. G. Novak, A. P. Tiwari, S. H. Song, B. Kim and S. Jeon, *Nano Lett.*, 2018, **18**, 5646–5651.

- 118 R. Li, K. Li, G. Wang, L. Li, Q. Zhang, J. Yan, Y. Chen, Q. Zhang, C. Hou, Y. Li and H. Wang, *ACS Nano*, 2018, **12**, 3759–3768.
- 119 H. Cui and M. Overend, *Energy Build.*, 2019, **199**, 427–444.
- 120 E. Sunada, K. Lankford, M. Pauken, K. S. Novak and G. Birur, *AIP Conf. Proc.*, 2002, **608**, 211–213.
- 121 G. Cha, C.-J. Kim and Y. S. Ju, *Appl. Therm. Eng.*, 2016, **98**, 189–195.
- 122 M. Dabbagh and M. Krarti, *Energy Build.*, 2020, **222**, 110025.
- 123 J. Fernández and R. Poulter, *Int. J. Heat Mass Transf.*, 1987, **30**, 2125–2136.
- 124 P. D. Shima and J. Philip, *J. Phys. Chem. C*, 2011, **115**, 20097–20104.
- 125 J. Philip, P. D. Shima and B. Raj, *Appl. Phys. Lett.*, 2008, **92**, 43108.
- 126 R. Baetens, B. P. Jelle and A. Gustavsen, *Sol. Energy Mater. Sol. Cells*, 2010, **94**, 87–105.
- 127 M. S. Dresselhaus and G. Dresselhaus, *Adv. Phys.*, 2002, **51**, 1–186.
- 128 J. S. Kang, M. Ke and Y. Hu, *Nano Lett.*, 2017, **17**, 1431–1438.
- 129 A. Sood, F. Xiong, S. Chen, H. Wang, D. Selli, J. Zhang, C. J. McClellan, J. Sun, D. Donadio, Y. Cui, E. Pop and K. E. Goodson, *Nat. Commun.*, 2018, **9**, 1–9.
- 130 Q. Lu, S. Huberman, H. Zhang, Q. Song, J. Wang, G. Vardar, A. Hunt, I. Waluyo, G. Chen and B. Yildiz, *Nat. Mater.*, 2020, **19**, 655–662.
- 131 S. Lee, K. Hippalgaonkar, F. Yang, J. Hong, C. Ko, J. Suh, K. Liu, K. Wang, J. J. Urban and X. Zhang, *Science*, 2017, **355**, 371–374.
- 132 K. Tang, X. Wang, K. Dong, Y. Li, J. Li, B. Sun, X. Zhang, C. Dames, C. Qiu, J. Yao and J. Wu, *Adv. Mater.*, 2020, **32**, 1907071.
- 133 R. Shrestha, Y. Luan, S. Shin, T. Zhang, X. Luo, J. S. Lundh, W. Gong, M. R. Bockstaller, S. Choi, T. Luo, R. Chen, K. Hippalgaonkar and S. Shen, *Sci. Adv.*, 2019, **5**, eaax3777.
- 134 J. Shin, J. Sung, M. Kang, X. Xie, B. Lee, K. M. Lee, T. J. White, C. Leal, N. R. Sottos, P. V. Braun and D. G. Cahill, *Proc. Natl. Acad. Sci. U. S. A.*, 2019, **116**, 5973–5978.
- 135 A. I. Volokitin and B. N. J. Persson, *Rev. Mod. Phys.*, 2007, **79**, 1291–1329.

- 136 S. Shen, A. Narayanaswamy and G. Chen, *Nano Lett.*, 2009, **9**, 2909–2913.
- 137 K. Kim, B. Song, V. Fernández-Hurtado, W. Lee, W. Jeong, L. Cui, D. Thompson, J. Feist, M. T. H. Reid and F. J. García-Vidal, *Nature*, 2015, **528**, 387–391.
- 138 D. Thompson, L. Zhu, E. Meyhofer and P. Reddy, *Nat. Nanotechnol.*, 2020, **15**, 99–104.
- 139 D. A. Broido, M. Malorny, G. Birner, N. Mingo and D. A. Stewart, *Appl. Phys. Lett.*, 2007, **91**, 67–70.
- 140 K. Esfarjani, G. Chen and H. T. Stokes, *Phys. Rev. B - Condens. Matter Mater. Phys.*, , DOI:10.1103/PhysRevB.84.085204.
- 141 L. Lindsay, C. Hua, X. L. Ruan and S. Lee, *Mater. Today Phys.*, 2018, **7**, 106–120.
- 142 J.-P. M. Péraud and N. G. Hadjiconstantinou, *Phys. Rev. B*, 2011, **84**, 205331.
- 143 J.-H. Lee, J. C. Grossman, J. Reed and G. Galli, *Appl. Phys. Lett.*, 2007, **91**, 223110.
- 144 T. Coquil, J. Fang and L. Pilon, *Int. J. Heat Mass Transf.*, , DOI:10.1016/j.ijheatmasstransfer.2011.06.024.
- 145 D. K. Bhamare, P. Saikia, M. K. Rathod, D. Rakshit and J. Banerjee, *Build. Environ.*, 2021, **199**, 107927.
- 146 W. Kohn and L. J. Sham, *Phys. Rev.*, 1965, **140**, A1133–A1138.
- 147 S. Baroni, S. de Gironcoli, A. Dal Corso and P. Giannozzi, *Rev. Mod. Phys.*, 2001, **73**, 515–562.
- 148 P. Giannozzi, S. Baroni, N. Bonini, M. Calandra, R. Car, C. Cavazzoni, D. Ceresoli, G. L. Chiarotti, M. Cococcioni, I. Dabo, A. Dal Corso, S. de Gironcoli, S. Fabris, G. Fratesi, R. Gebauer, U. Gerstmann, C. Gougoussis, A. Kokalj, M. Lazzeri, L. Martin-Samos, N. Marzari, F. Mauri, R. Mazzarello, S. Paolini, A. Pasquarello, L. Paulatto, C. Sbraccia, S. Scandolo, G. Sclauzero, A. P. Seitsonen, A. Smogunov, P. Umari and R. M. Wentzcovitch, *J. Phys. Condens. Matter*, 2009, **21**, 395502.
- 149 W. Li, J. Carrete, N. A. Katcho and N. Mingo, *Comput. Phys. Commun.*, 2014, **185**, 1747–1758.
- 150 A. Togo and I. Tanaka, *Scr. Mater.*, 2015, **108**, 1–5.
- 151 H. Wu, H. Fan and Y. Hu, *Phys. Rev. B*, 2021, **103**, L041203.
- 152 H. Fan, H. Wu, L. Lindsay and Y. Hu, *Phys. Rev. B*, 2019, **100**, 85420.



- 153 J. S. Kang, H. Wu and Y. Hu, *Nano Lett.*, 2017, **17**, 7507–7514.
- 154 J. S. Kang, M. Li, H. Wu, H. Nguyen and Y. Hu, *Science*, 2018, **361**, 575–578.
- 155 Y. Cui, Z. Qin, H. Wu, M. Li and Y. Hu, *Nat. Commun.*, 2021, **12**, 1284.
- 156 J. S. Kang, M. Li, H. Wu, H. Nguyen, T. Aoki and Y. Hu, *Nat. Electron.*, 2021, **4**, 416–423.
- 157 J. M. Larkin and A. J. H. McGaughey, *Phys. Rev. B - Condens. Matter Mater. Phys.*, 2014, **89**, 144303.
- 158 H. R. Seyf and A. Henry, *J. Appl. Phys.*, 2016, **120**, 25101.
- 159 C. L. Tien, *Microscale Energy Transfer*, Taylor & Francis, 1997.
- 160 Y. Cui, M. Li and Y. Hu, *J. Mater. Chem. C*, 2020, **8**, 10568–10586.
- 161 M. Li, J. S. Kang, H. D. Nguyen, H. Wu, T. Aoki and Y. Hu, *Adv. Mater.*, 2019, **31**, 1901021.
- 162 X. Lu, P. Wang, M. C. Arduini-Schuster, J. Kuhn, D. Büttner, O. Nilsson, U. Heinemann and J. Fricke, *J. Non. Cryst. Solids*, 1992, **145**, 207–210.
- 163 G. H. Tang, C. Bi, Y. Zhao and W. Q. Tao, *Energy*, 2015, **90**, 701–721.
- 164 L. W. Hrubesh and R. W. Pekala, *J. Mater. Res.*, 1994, **9**, 731–738.
- 165 Y. Yan, M. Li, S. King, T. Galy, M. Marszewski, J. S. Kang, L. Pilon, Y. Hu and S. H. Tolbert, *J. Phys. Chem. Lett.*, 2020, **11**, 3731–3737.
- 166 A. L. Moore and L. Shi, *Mater. Today*, 2014, 163–174.
- 167 E. T. Swartz and R. O. Pohl, *Rev. Mod. Phys.*, 1989, **61**, 605.
- 168 M. Büttiker, *Phys. Rev. B*, 1988, **38**, 9375.
- 169 Y. Zhao, G. H. Tang and M. Du, *Int. J. Therm. Sci.*, 2015, **89**, 110–120.
- 170 M. Bartak, I. Beausoleil-Morrison, J. A. Clarke, J. Denev, F. Drkal, M. Lain, I. A. Macdonald, A. Melikov, Z. Popiolek and P. Stankov, *Build. Environ.*, 2002, **37**, 865–871.
- 171 K. T. Butler, D. W. Davies, H. Cartwright, O. Isayev and A. Walsh, *Nature*, 2018.
- 172 P. Raccuglia, K. C. Elbert, P. D. F. Adler, C. Falk, M. B. Wenny, A. Mollo, M. Zeller, S. A. Friedler, J. Schrier and A. J. Norquist, *Nature*, 2016, **533**, 73–76.
- 173 P. Nath, J. J. Plata, D. Usanmaz, C. Toher, M. Fornari, M. B. Nardelli and S. Curtarolo, *Scr.*

- Mater.*, 2017, **129**, 88–93.
- 174 L. Chen, H. Tran, R. Batra, C. Kim and R. Ramprasad, *Comput. Mater. Sci.*, 2019, **170**, 109155.
- 175 C. Toher, J. J. Plata, O. Levy, M. De Jong, M. Asta, M. B. Nardelli and S. Curtarolo, *Phys. Rev. B*, 2014, **90**, 174107.
- 176 H. Zhang, K. Hippalgaonkar, T. Buonassisi, O. M. L. Løvvik, E. Sagvolden and D. Ding, *ES Energy Environ.*, 2018, 2, 1–8.
- 177 J. Carrete, W. Li, N. Mingo, S. Wang and S. Curtarolo, *Phys. Rev. X*, 2014, **4**, 11019.
- 178 R. Juneja, G. Yumnam, S. Satsangi and A. K. Singh, *Chem. Mater.*, 2019, **31**, 5145–5151.
- 179 P. Roy Chowdhury, C. Reynolds, A. Garrett, T. Feng, S. P. Adiga and X. Ruan, *Nano Energy*, 2020, **69**, 104428.
- 180 Y.-J. Wu, L. Fang and Y. Xu, *npj Comput. Mater.*, 2019, **5**, 1–8.

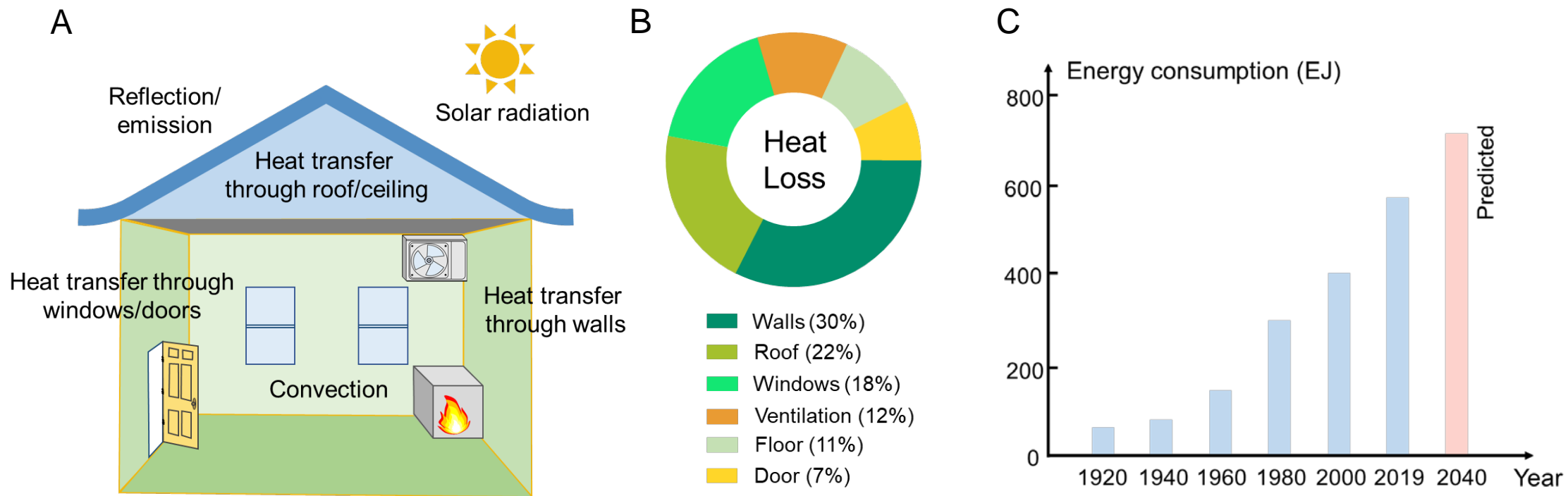


Figure 1

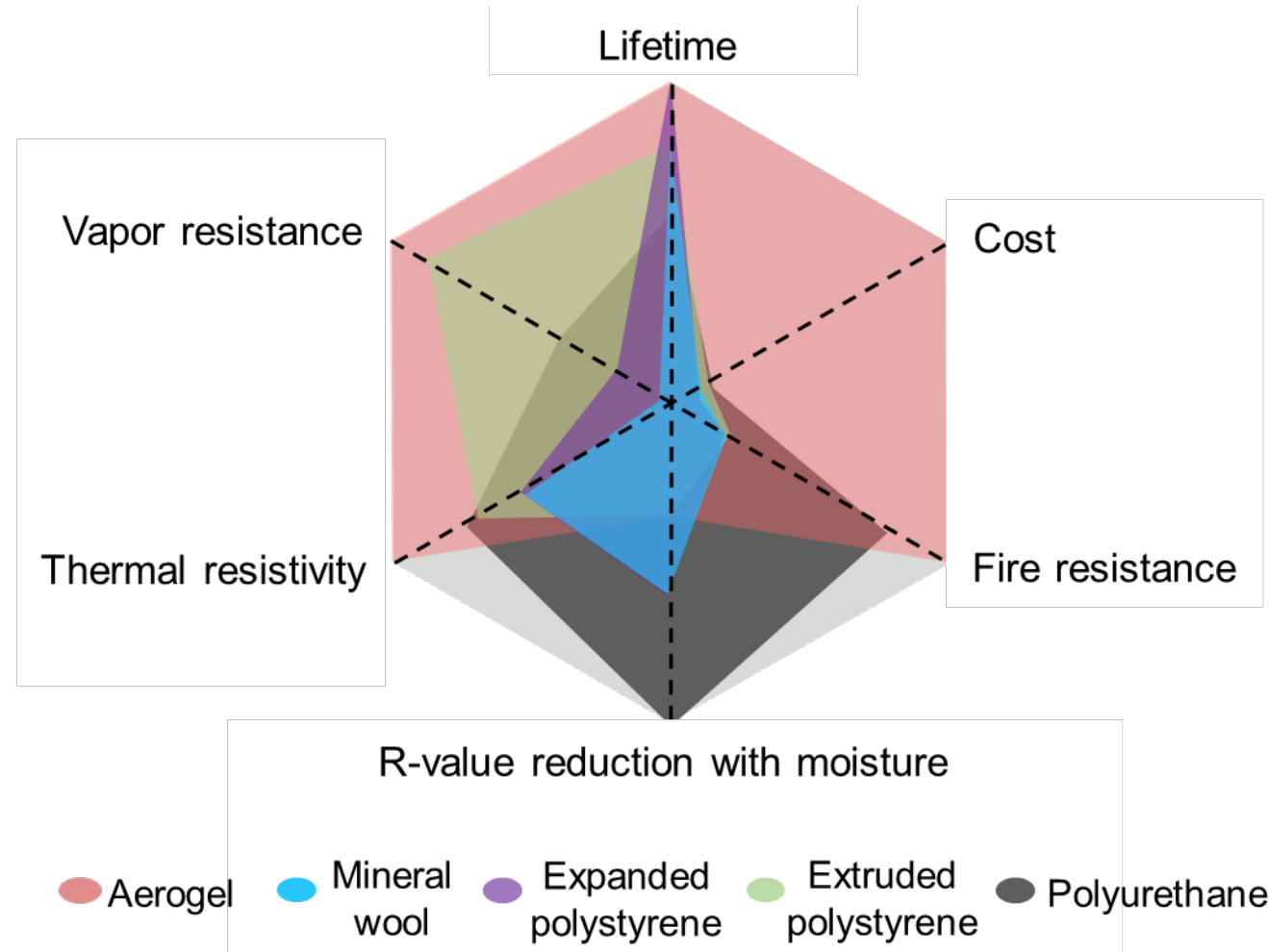


Figure 2

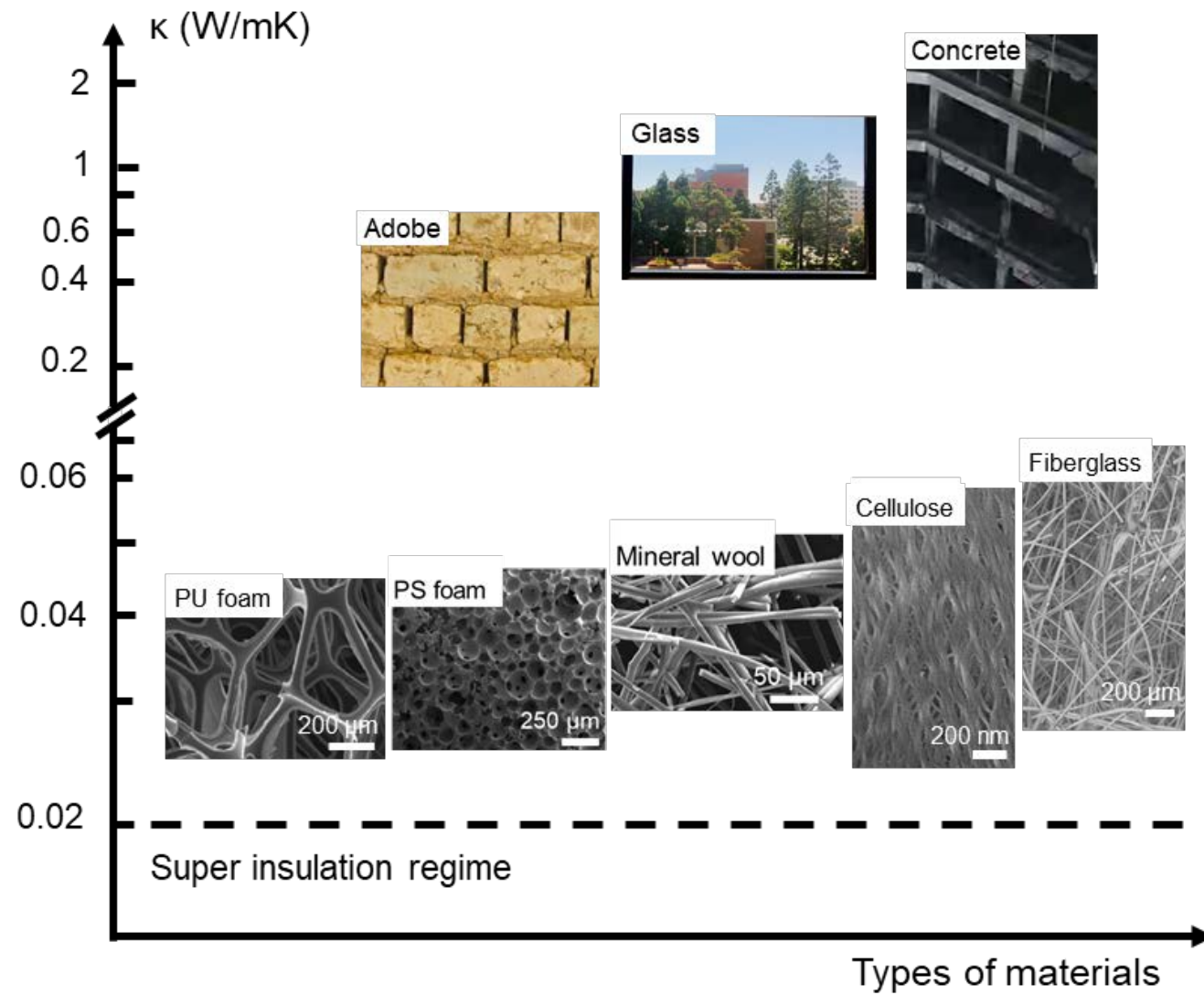


Figure 3

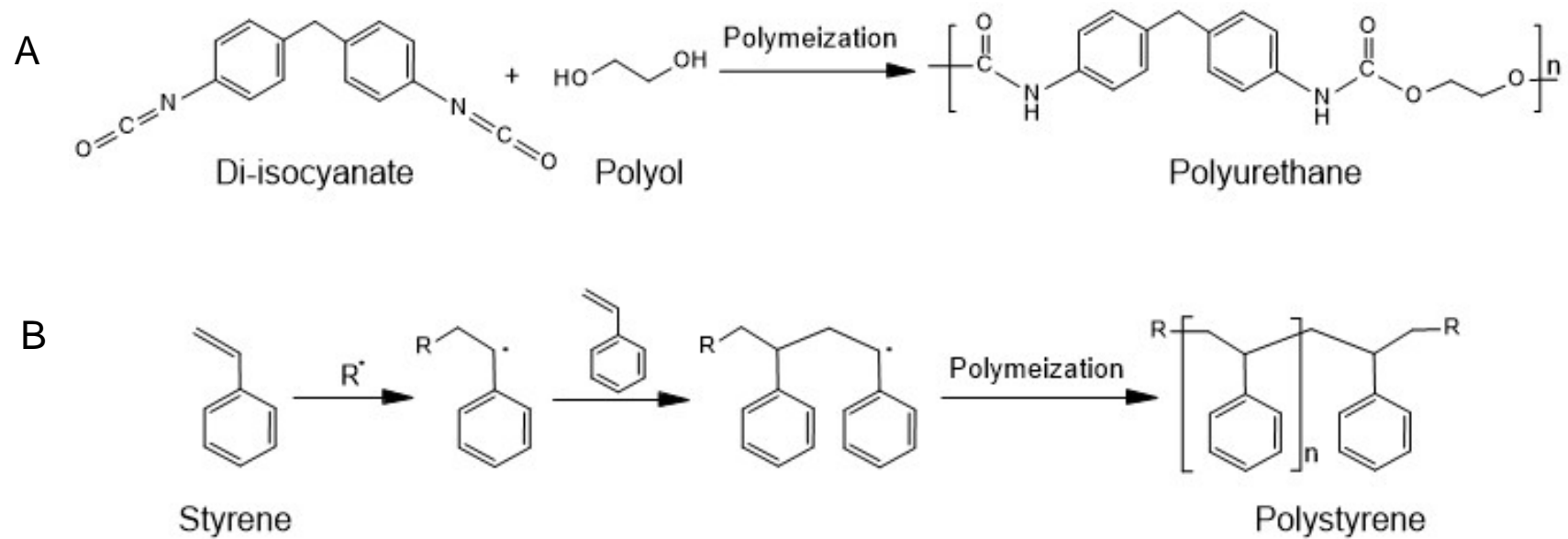


Figure 4

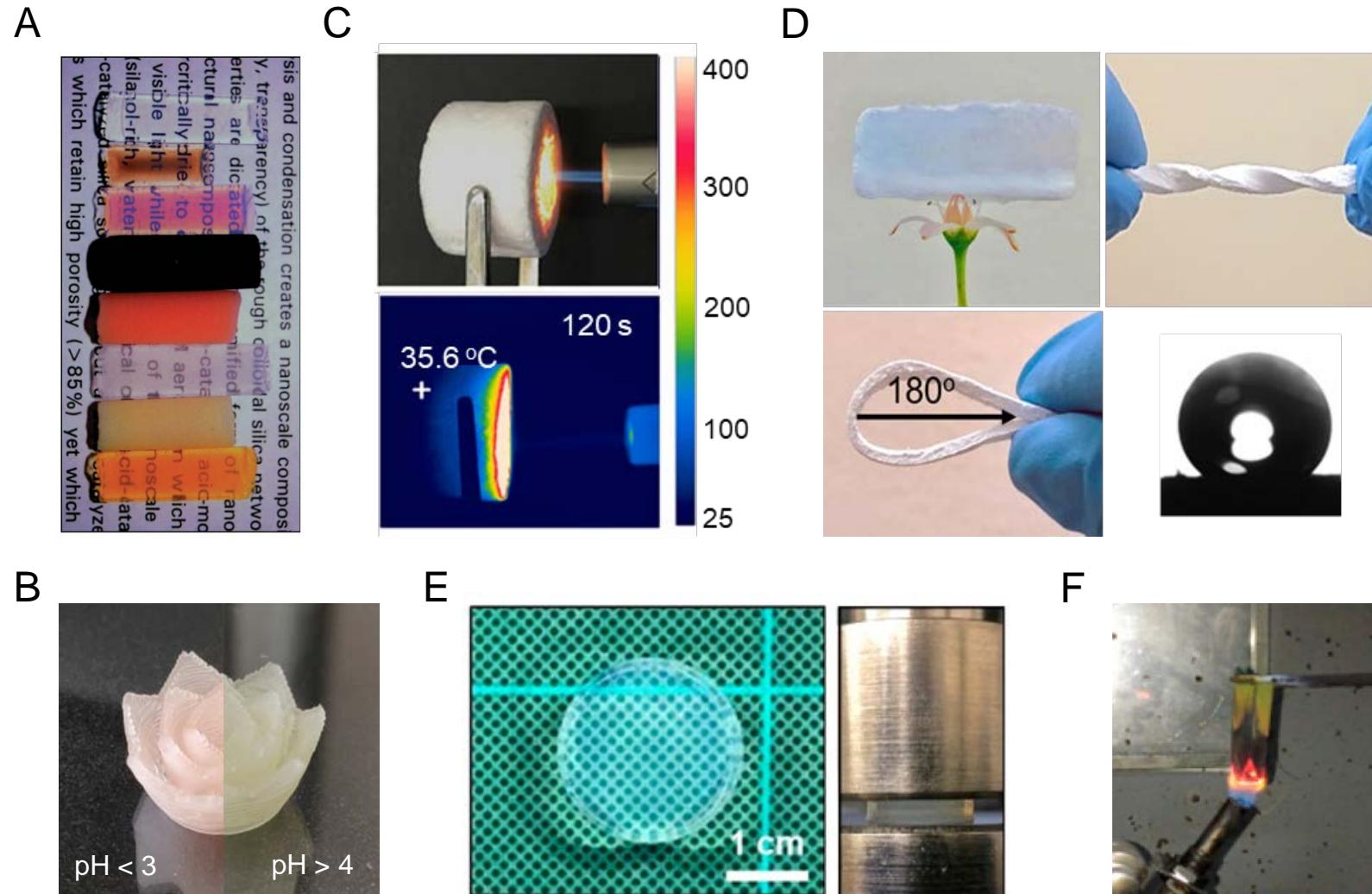


Figure 5

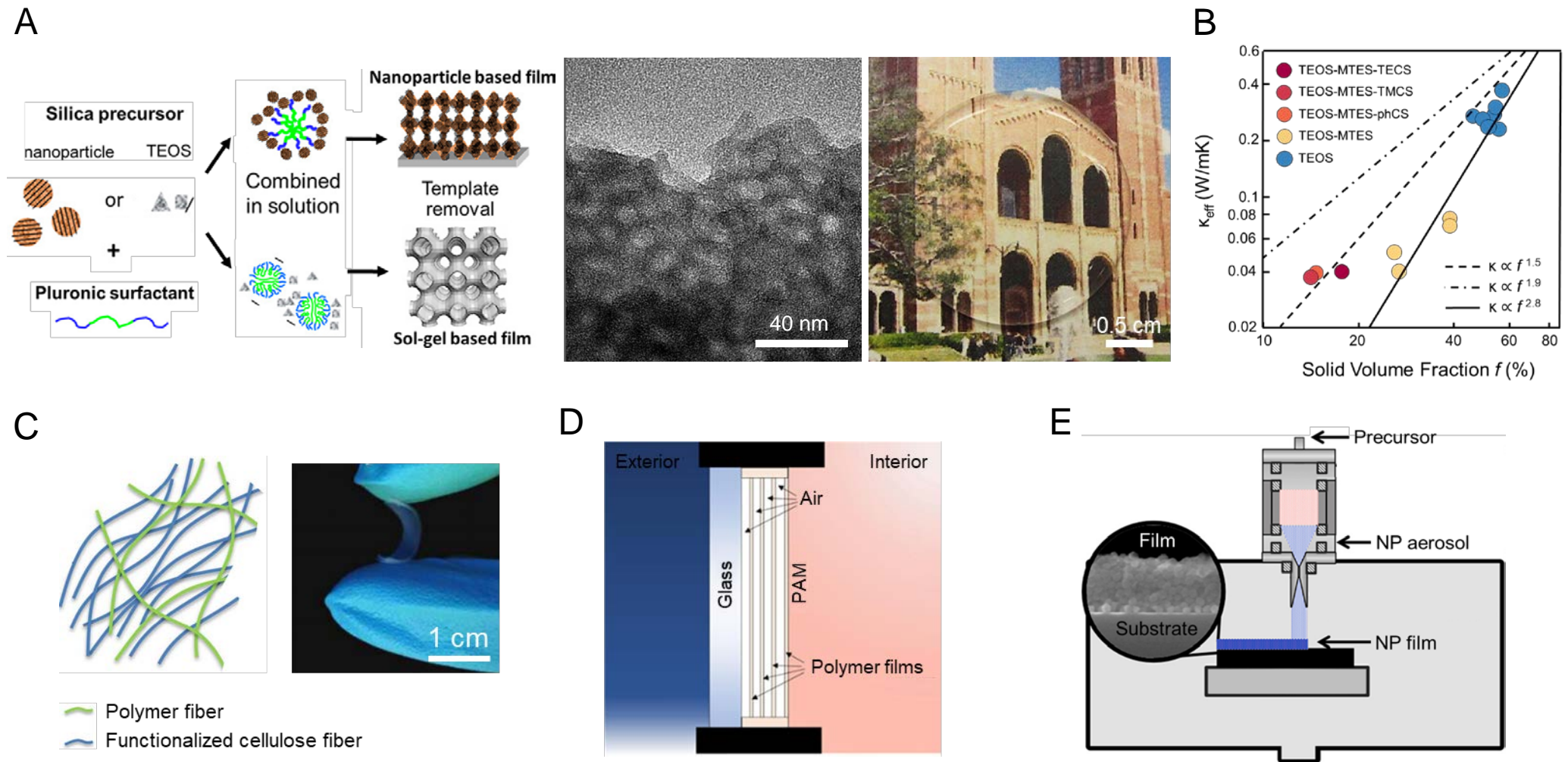
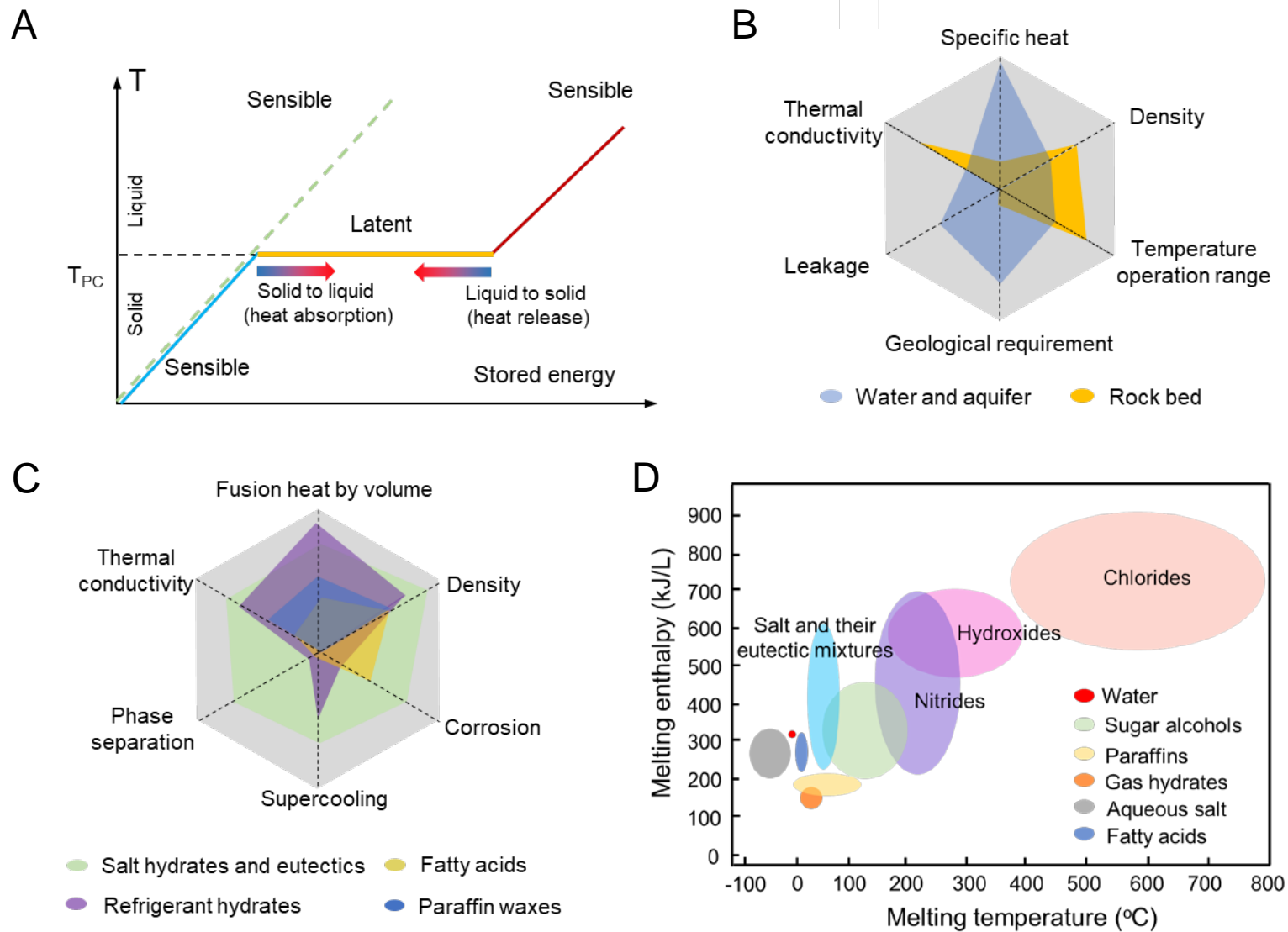


Figure 6





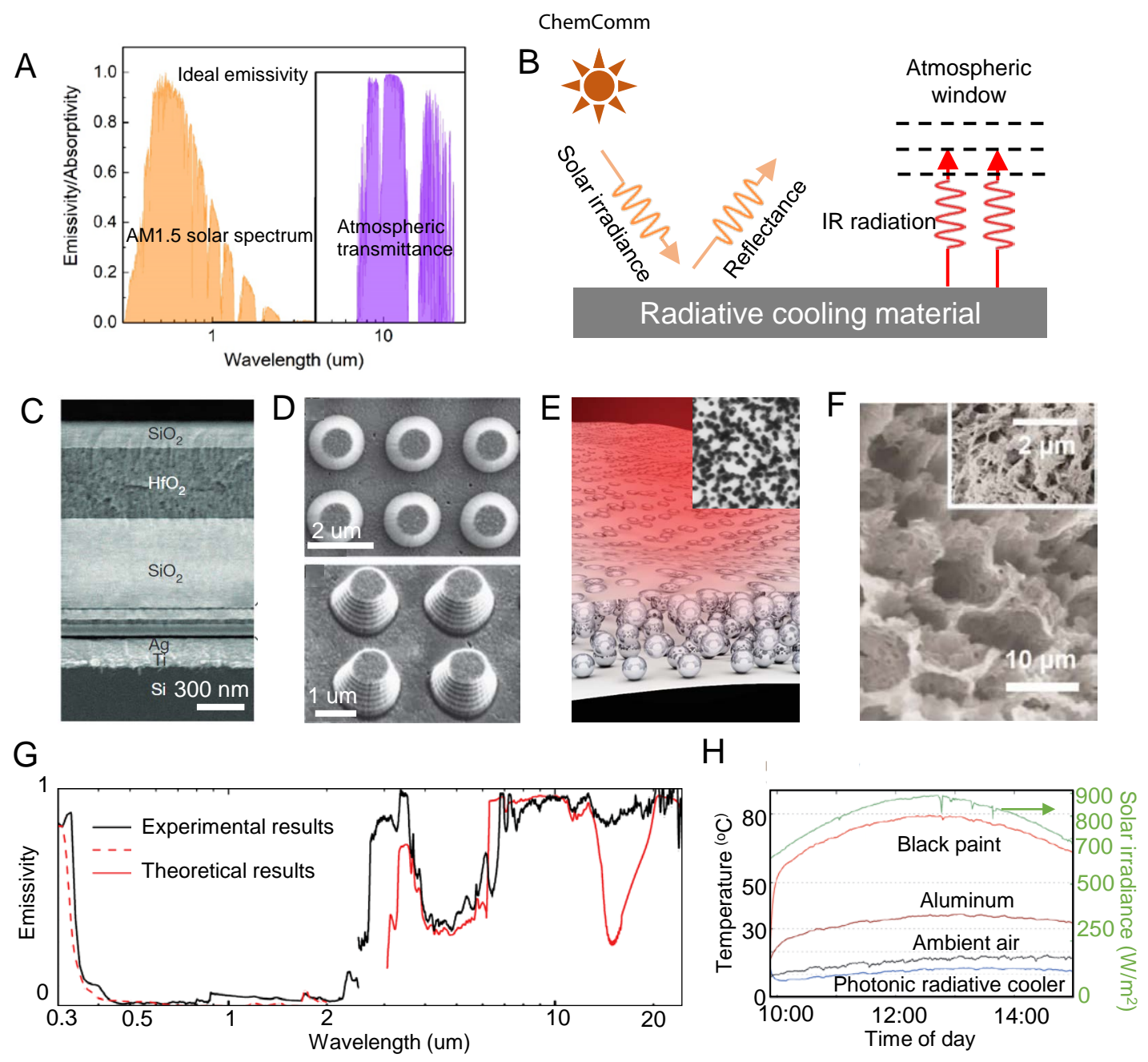
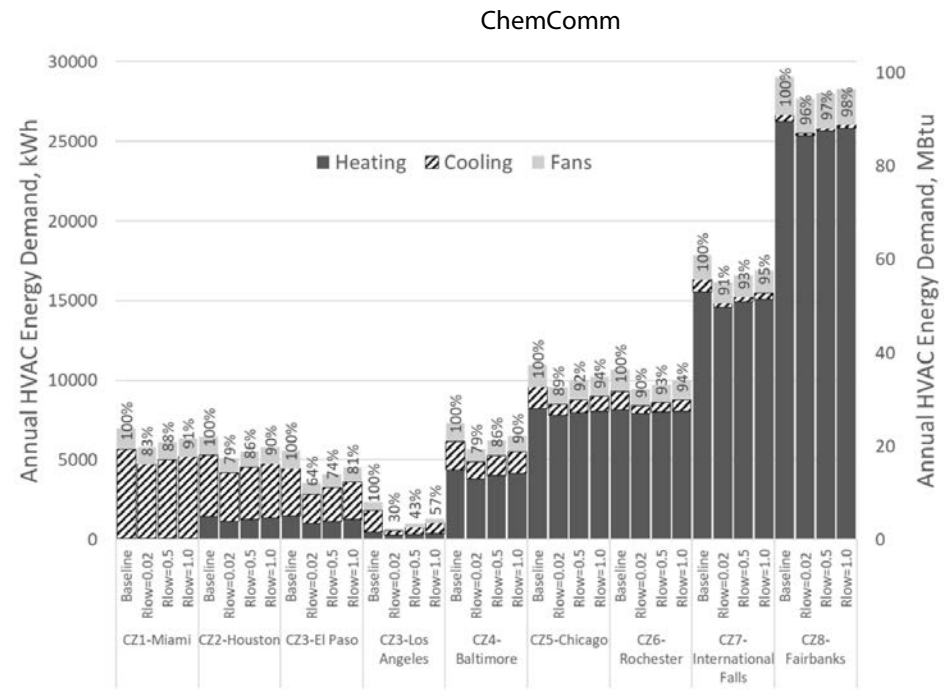


Figure 8

A



B

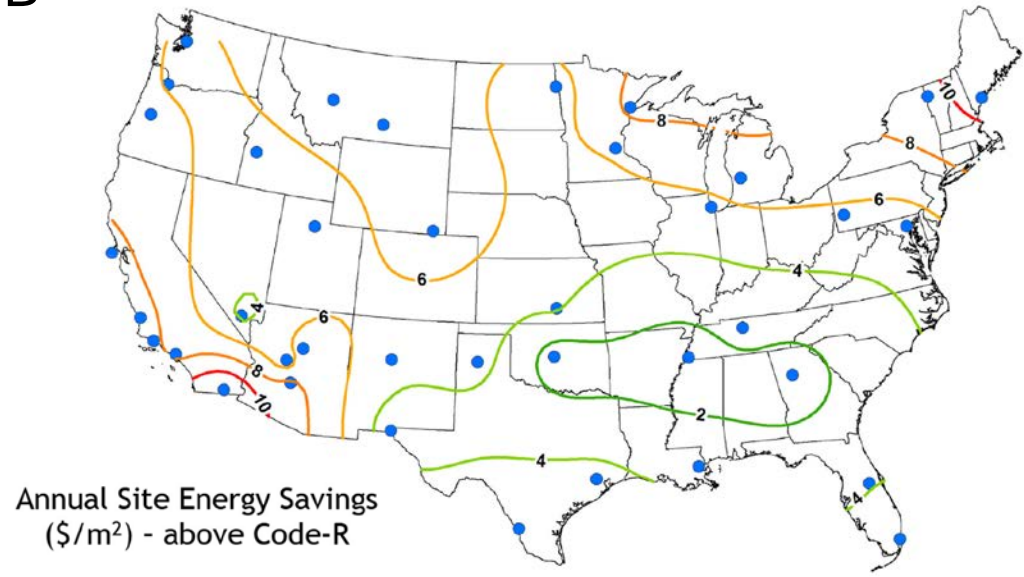


Figure 9

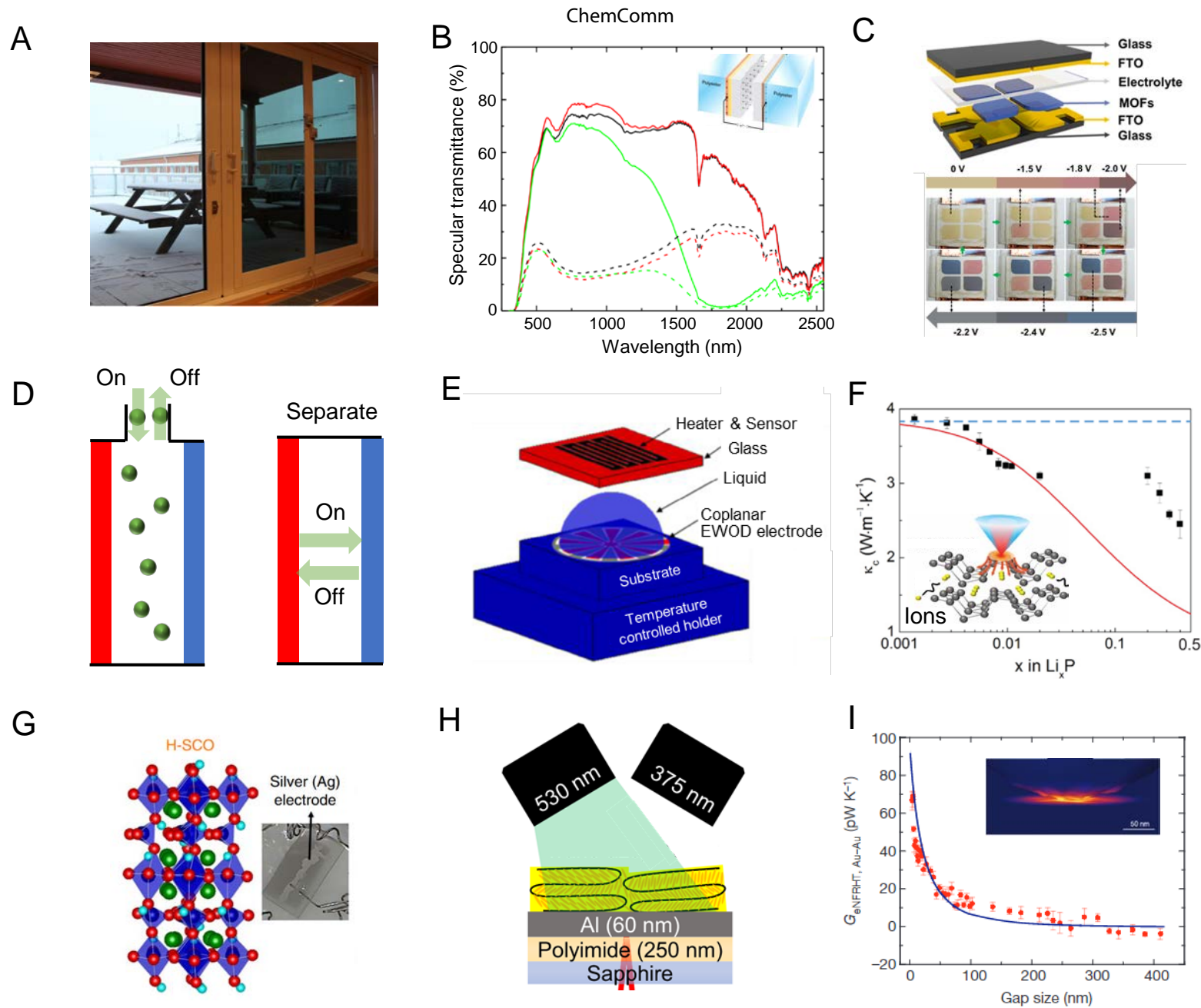


Figure 10

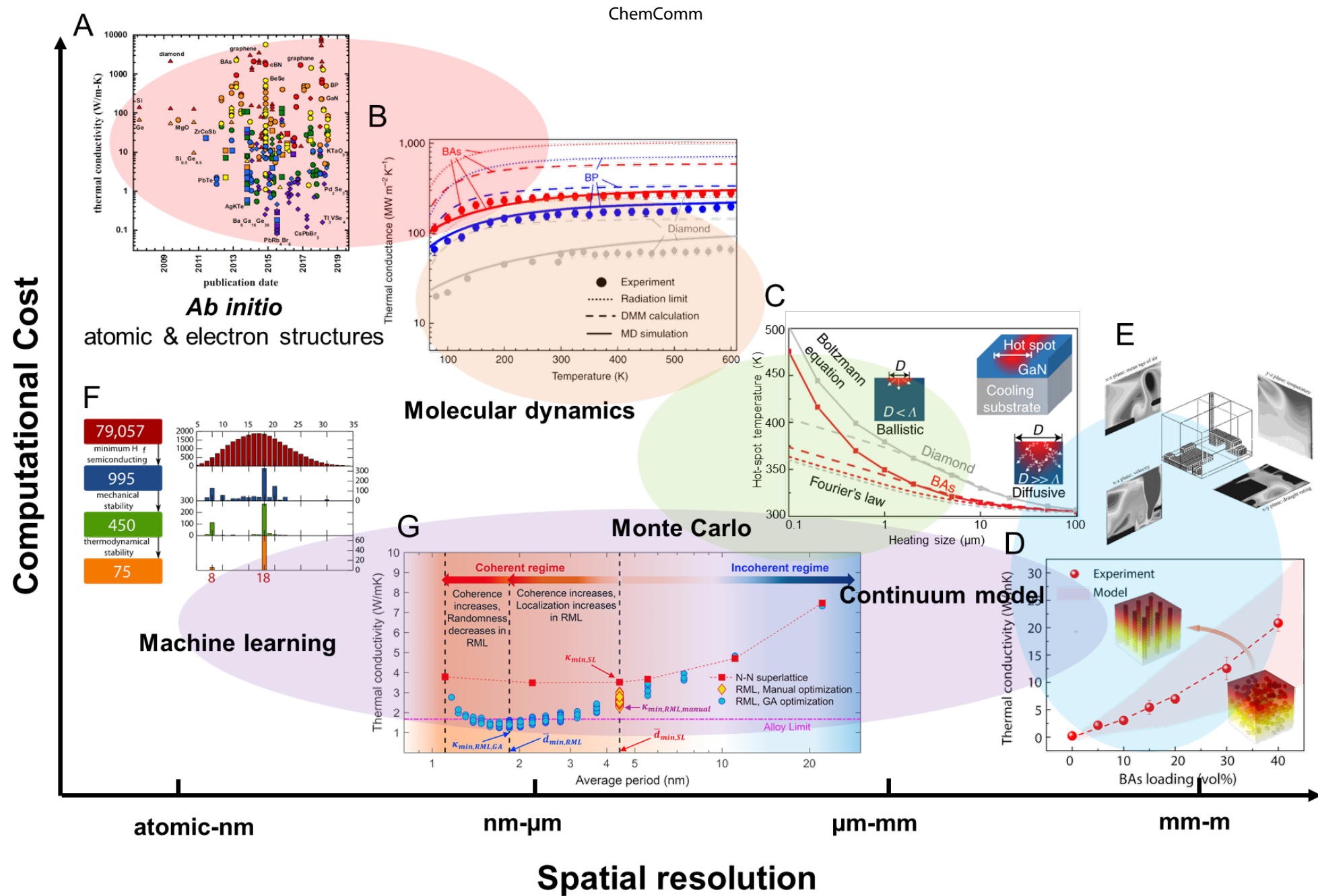


Figure 11